

THERMAL MANAGEMENT TECHNOLOGIES OF LITHIUM-ION BATTERIES APPLIED FOR STATIONARY ENERGY STORAGE SYSTEMS

Investigation on the thermal behavior of Lithium-ion batteries

HAIDER ADEL ALI ALI

ZIAD NAMIR ABDELJAWAD

School of Business, Society and Engineering

Course: Degree Project in Energy Engineering

Course code: ERA403

Credits: 30 hp

Program: Master of Science in Engineering-
Energy Systems

Supervisor at Mälardalens University: Hailong Li

Supervisor at Vattenfall R&D: Jinying Yan

Examiner: Jan Sandberg

Date: 2020-06-14

E-post:

hai15003@student.mdh.se

zad15002@student.mdh.se

ABSTRACT

Batteries are promising sources of green and sustainable energy that have been widely used in various applications. Lithium-ion batteries (LIBs) have an important role in the energy storage sector due to its high specific energy and energy density relative to other rechargeable batteries. The main challenges for keeping the LIBs to work under safe conditions, and at high performance are strongly related to the battery thermal management. In this study, a critical literature review is first carried out to present the technology development status of the battery thermal management system (BTMS) based on air and liquid cooling for the application of battery energy storage systems (BESS). It was found that more attention has paid to the BTMS for electrical vehicle (EV) applications than for stationary BESS. Even though the active forced air cooling is the most commonly used method for stationary BESS, limited technical information is available. Liquid cooling has widely been used in EV applications with different system configurations and cooling patterns; nevertheless, the application for BESS is hard to find in literature.

To ensure and analyze the performance of air and liquid cooling system, a battery and thermal model developed to be used for modeling of BTMS. The models are based on the car company BMW EV battery pack, which using Nickel Manganese Cobalt Oxide (NMC) prismatic lithium-ion cell. Both air and liquid cooling have been studied to evaluate the thermal performance of LIBs under the two cooling systems.

According to the result, the air and liquid cooling are capable of maintaining BESS under safe operation conditions, but with considering some limits. The air-cooling is more suitable for low surrounding temperature or at low charging/discharge rate (C-rate), while liquid cooling enables BESS to operate at higher C-rates and higher surrounding temperatures. However, the requirement on the maximum temperature difference within a cell will limits the application of liquid cooling in some discharge cases at high C-rate. Finally, this work suggests that specific attention should be paid to the pack design. The design of the BMW pack is compact, which makes the air-cooling performance less efficient because of the air circulation inside the pack is low and liquid cooling is more suitable for this type of compact battery pack.

Keywords: Air and liquid cooling, battery thermal management system, Lithium-ion batteries, NMC, prismatic cell, pack simulation, maximum temperature difference, charging/discharging rates, thermal behavior, thermal modeling/simulation

PREFACE

This study is a degree project in Master of Science in Engineering Energy systems at Mälardalens University in Sweden, written by Haider Adel Ali and Ziad Namir Abdeljawad during the spring semester 2020. We want to send many thanks to Vattenfall for the support to conduct this thesis.

We would also like to express our gratitude to our supervisors Jinying Yan, professor at Vattenfall R&D, and KTH, and Hailong Li, Senior Lecturer and Associate Professor at Mälardalens University. Special thanks to Firas Alhaider, Engineer at Vattenfall, for the guidance and support during this period and the rest of the colleges at Vattenfall. Finally, we would like to thank our examiner at Mälardalens university Jan Sandberg, Senior Lecturer, for the feedback and support.

Stockholm, Sweden, 2020

Haider Adel Ali and Ziad Namir Abdeljawad

SUMMARY

Lithium-ion batteries (LIBs) are gaining momentum as a suitable and sustainable alternative to be used in electric vehicle (EV) and battery energy storage system (BESS). The performance, safety, and lifetime of LIBs are highly dependent on the internal operating cell temperature, which makes the thermal characterization of battery cells necessary and a critical factor. Therefore, understanding the thermal effects is very vital towards developing and selecting proper battery thermal management systems (BTMS).

The project aims to investigate the status of the development of BTMS applied for stationary lithium-ion BESS and compare the performances of BTMS using air and liquid cooling. A battery and thermal model were developed to study the thermal behavior of specific battery cell and used for modeling of BTMS (air and liquid cooling). Furthermore, the performance of the two cooling systems was simulated and compared.

The cell studied in this work is a 120 Ah prismatic type with Nickel Manganese Cobalt Oxide (NMC) chemistry. The battery model was developed using equivalent circuit modeling (ECM). The model was simplified, and two resistance-capacitor parallel network ECM was developed in MATLAB-Simulink. Parameter identification for the ECM was conducted with a pulse test and a low current experiment. The thermal model of the cell was developed based on a lumped system analysis. The model was validated against experimental data, and the average root-mean-square deviation (RMSE) on temperature was 0.38°C which indicates that the model is accurate.

The cell model was then integrated into a battery pack model based on the car company BMW battery pack used for their EV. The pack model was then used for simulation of the thermal performance of the BTMS to maintain the appropriate temperature of the battery. The battery pack is equipped with a cooling plate using R134a refrigerant placed on the bottom side of the battery modules inside the pack. The liquid cooling can be turned off, and the pack is only cooled with passive air cooling. The pack BTMS model was developed and validated against operation data. The result of the validation shows that the average RMSE on temperature is about 1°C for both air and liquid cooling.

The battery temperature was studied under air and liquid cooling to compare their performance. A study was also conducted to investigate the influence of the surrounding temperature, which varied between 12 and 32°C . According to literature, the optimum temperature for LIB should be between 15 and 35°C , and the maximum temperature difference in the cell should not exceed 5 degrees in order to keep the cell in good condition and have the expected lifetime. Based on these, simulation results show that air cooling has the advantage of operating between the surrounding temperature below 18°C at discharge. However, for all the other temperature cases, liquid cooling performance better and can be operating at higher surrounding temperature cases with higher C-rate. Furthermore, the result shows that the allowed maximum cell temperature difference has some certain limitations when using liquid cooling in most of the discharge cases.

In literature shows that there is more study about the BTMS used for EV applications, but according to the literature, the major BTMS applied for stationary applications used an air-

cooling system. Considering air cooling, the BMW battery pack is compact, and there are no gaps between each cell for the air to flow through, resulting in low air circulation inside the pack. This makes the BMW pack not a good design with passive air cooling. In future work, a more air-cooling design pack will be studied to give a more comparable comparison between the BMW air and liquid cooling with other manufacturers.

Another suggestion for future work is to integrate the aging factor in the model. This can make the model capable of studying cell capacity degradation to reckon a cell's lifetime. Finally, the computational fluid dynamics (CFD) model of the pack can be developed to study the heat flow and air circulation in the pack in more detail.

TABLE OF CONTENTS

1	INTRODUCTION	12
1.1	Background	12
1.2	Problem Statement.....	13
1.3	Purpose.....	13
1.4	Research questions	14
1.5	Delimitation.....	14
2	METHODOLOGY	15
2.1	Literature review.....	15
2.2	Battery Thermal modeling	15
2.3	Battery Thermal Management system	15
3	LITERATURE STUDY	16
3.1	Lithium-ion battery	16
3.1.1	Lithium-ion batteries common chemistries	17
3.1.2	Key performance of commercial LIBS with different formats	18
3.1.2.1.	<i>Cylindrical cell</i>	19
3.1.2.2.	<i>Pouch cell</i>	19
3.1.2.3.	<i>Prismatic cell</i>	20
3.2	Battery models review.....	20
3.2.1	Overview of battery models.....	20
3.2.1.1	<i>Electrochemical Model</i>	20
3.2.1.2	<i>Stochastic Model</i>	20
3.2.1.3	<i>Neural network models</i>	21
3.2.1.4	<i>Peukert's law model</i>	21
3.2.1.5	<i>Equivalent Circuit model</i>	21
3.2.2	Summary of battery models	21
3.2.3	Selection of battery model.....	22
3.3	Battery thermal models review	23
3.3.1.1	<i>Lumped capacitance thermal model</i>	23
3.3.1.2	<i>Partial differential equations models</i>	23
3.3.1.3	<i>Finite element analysis battery thermal model</i>	23
3.3.2	Summary of thermal models	24
3.3.3	Selection of battery thermal model	24
3.4	Main thermal issues and impacts of commercial LIBs	24
3.4.1	Performance degradation.....	25

3.4.2	Low-temperature effects	25
3.4.3	Thermal Runaway	26
3.4.4	Temperature distribution	27
3.5	Handling thermal issues and impacts of commercial LIBs	27
3.6	Cooling systems applied for LIBs	28
3.6.1	Air cooling	29
3.6.2	Liquid cooling	31
3.6.3	Comparison between air and liquid cooling system	32
4	CASE STUDIES	35
4.1	Battery Model	36
4.1.1	Parameter Identification	38
4.1.2	Parameter estimation	39
4.1.3	Experiments	39
4.1.3.1	<i>Pulse test</i>	39
4.1.3.2	<i>Low current experiment</i>	40
4.2	Battery Thermal Model	42
4.2.1	Heat generation in Lithium-ion Batteries	42
4.2.2	Heat transfer model in the Cell	44
4.2.3	Cell Thermal Model Validation	47
4.3	BTMS	49
4.3.1	Pack Model Validation	51
4.3.1.1	<i>Air Cooling Validation</i>	51
4.3.1.2	<i>Liquid Cooling Validation</i>	53
5	RESULTS	55
5.1	Cell terminal voltage	55
5.2	Cell heat generation	56
5.3	Simulation result for BTMS	57
5.3.1	Air cooling	57
5.3.2	Liquid cooling	59
5.3.3	Comparison between Air and Liquid cooling	62
5.3.4	Relaxing period	62
6	DISCUSSION	64
7	CONCLUSION	66

8 FUTURE WORK	67
APPENDIX 1: OCV MEASUREMENT	75
APPENDIX 2: OPERATION DATA VALIDATION	76
APPENDIX 3: SCREENSHOTS OF THE MODEL IN SIMULINK.....	80

LIST OF FIGURES

Figure 1 Lithium-ion battery typical component.	16
Figure 2 Technical differences and similarities between the most common cell types chemistries. (Battery university, 2019).	17
Figure 3 Compression between different lithium-ion cell designs. (Hannan, Hoque, Hussain, Yusof, & Ker, 2018) (Battery university, 2019) (relionbattery, 2019) (E.Ciez & J.F., 2017) (Miao, Hynan, Von Jouanne, & Yokochi, 2019).	18
Figure 4 Calendar aging behaviors of three common LIB cells (Schuster, o.a., 2016).	25
Figure 5 Nominal operation condition for the lithium-ion cells (Wiebelt, 2018).	28
Figure 6 Thermal management using air cooling (left) and liquid cooling (right) (Zhonghao & Shuangfeng, 2011).	29
Figure 7 General KPI for both air and liquid cooling systems. (Chen, Jiang, Kim, Yang, & Pesaran, 2016), (Kim, Ho, Marina, & Eugene, 2012), (Han, Khalighi, & Kaushik, 2017), (Khan, Nielsen, & Kær, 2014), (Madani, Swierczynski, & Kær, 2017).	33
Figure 8 General equivalent circuit model.	36
Figure 9 Simplified ECM for lithium-ion batteries with two RC parallel networks and neglectation of the parasitic branch.	37
Figure 10 Flow diagram of parameter estimation.	38
Figure 11 Data correlation to the ECM.	39
Figure 12 Measured data from pulse test for 40°C discharge.	40
Figure 13 Measured data from low current experiment for 40°C discharge.	41
Figure 14 Entropic coefficients as a function of SOC.	43
Figure 15 Heat dissipation between the irreversible and reversible as a function of C-rate. ..	43
Figure 16 Cell heat rate as a function of SOC with operation C-rate at 0.5 and temperature around 25 °C.	44
Figure 17 Schematic figure of the cell component, cell front (left), and cell side (right).	45
Figure 18 Lumped thermal model of the cell.	46
Figure 19 Coupling between the ECM, thermal model, and surrounding.	47
Figure 20 Methodology for cell thermal model validation.	48
Figure 21 Cell model validation methodology.	48
Figure 22 Battery pack used for the BTMS study (Dipl.-Ing. Florian Schoewel, 2013).	49

Figure 23 Battery module setup.....	50
Figure 24 BMTS Pack model validation methodology.....	51
Figure 25 Air cooling temperature validation discharge	52
Figure 26 Air cooling temperature validation charge.....	52
Figure 27 Liquid cooling temperature validation.	53
Figure 28 Voltage curve with C-rate for 0 °C, discharge (left), and charge (right).	55
Figure 29 Voltage curve with C-rate for 25 °C, discharge (left), and charge (right).	56
Figure 30 Voltage curve with C-rate for 40 °C, discharge (left), and charge (right).	56
Figure 31 Cell heat generation for different C-rate with cell temperature, discharge (left) and charge (right).....	57
Figure 32 Max temperature of the cell using air cooling, discharge (left), and charge (right).	58
Figure 33 Temperature difference between the initial and max temperature of the cell for air cooling, discharge (left), and charge (right).....	59
Figure 34 Max temperature difference between different parts in the of the cell for air cooling, discharge (left), and charge (right).....	59
Figure 35 Max temperature of the cell using liquid cooling, discharge (left), and charge (right).	60
Figure 36 Temperature difference between the initial and max temperature of the cell for liquid cooling, discharge (left), and charge (right).	61
Figure 37 Max temperature difference between different parts in the of the cell for liquid cooling discharge (left), and charge (right).....	61
Figure 38 Relaxing period simulation.....	63

LIST OF TABLES

Table 1 Properties for the different Lithium-ion cell chemistries. (Battery university, 2019) .	17
Table 2 The most common cell properties concerning industrial applications (Miao, Hynan, Von Jouanne, & Yokochi, 2019), (Battery university, 2019).....	19
Table 3 Battery models summary.	22
Table 4 Battery thermal models summary.....	24
Table 5 Summary of the air-cooling system used in industrial applications for BTMS.	30
Table 6 Summary of the liquid-cooling system used in industrial applications for BTMS.	32
Table 7 Advantages and disadvantages of the liquid cooling systems. (Maan, Ibrahim, & Marc A, 2018), (S.Panchal, o.a., 2017), (Qian, Li, & Rao, 2016), (E, o.a., 2018),	33
Table 8 Advantages and disadvantages of the air-cooling systems. (Lip, o.a., 2016), (Zhoujian, Li, Yong, Chao, & Xuejiao, 2017), (Chen, Jiang, Kim, Yang, & Pesaran, 2016), (Chen, Jiang, Kim, Yang, & Pesaran, 2016).	34
Table 9 General technical specifications of the cell	35
Table 10 Symbols description of ECM of the cell.....	36

Table 11 OCV Initial and End.	41
Table 12 Symbols description of heat transfer equations.	45
Table 13 Symbols description of the lumped thermal model of the cell.	46
Table 14 General technical specifications of the pack.	49
Table 15 Pack material and specifications	50
Table 16 Battery cooling system specifications	50
Table 17 Air cooling model validation.	53
Table 18 Liquid cooling model validation.	54
Table 19 Operation condition for air cooling.	58
Table 20 Operation condition for liquid cooling.	60
Table 21 Operation condition for liquid cooling after ΔT cell.	62
Table 22 Comparison between liquid and air cooling.	62
Table 23 Cases cooling time from 32 to 23 °C	63

NOMENCLATURE

Symbol	Description	Unit
A	Area	m ²
C	Capacitance	F
C _{capacity}	Battery cell capacity	Ah
C _N	Rated stored battery capacity	Ah
C _{th}	Thermal mass capacity	J/K
E	Energy	Wh or J
h	Heat transfer coefficient	W/m ² , K
I	Electric current	A
k	Thermal conductivity	W/m, K
L	Length	m
Q	Heat	W
R	Resistance	Ω
R _{th}	Thermal resistance	K/W
T	Temperature	°C or K
t	Time	s or h
V	Voltage	V
Z _p	Impedance of parasitic branch	Ω
Δ	Delta	-
η	Efficiency	%

ABBREVIATIONS AND TERMS

Abbreviation	Description
BESS	Battery Energy Storage System
BMS	Battery management system
BTMS	Battery Thermal Management System
CE	Coulombic efficiency
CFD	Computational fluid dynamics
DOD	Depth of discharge
ECM	Equivalent circuit model
E_m	Electromotive force
EV	Electric vehicle
HVAC	Heat ventilation air conditioner
KPI	Key performance indicators
LFP	Lithium Iron Phosphate Lithium Nickel
LIB	Lithium-ion battery
NCA	Lithium Nickel Cobalt Aluminum Oxide
NMC	Lithium Nickel Manganese Cobalt Oxide
OCV	Open-circuit Voltage
PDE	Partial differential equations
R^2	Coefficient of determination
RMSE	Root-mean-square deviation
SEI	Solid electrolyte interphase
SOC	State of charge
t_0	Initial state
TR	Thermal runaway

DEFINITIONS

Definition	Description
Anode	The anode is the positively charged electrode
Cathode	The cathode is the negatively charged electrode
C-rate	The C-rate is a measure of the rate at which a battery is being discharged/charged

1 INTRODUCTION

Renewable energy sources have a great benefit that gives a sustainable power generation with concern on as little impact on the environment as possible. The rise of power generation from renewable energy sources in the current energy market has resulted in the immense potential for different forms of energy storage, most likely a battery energy storage system (BESS). The BESS provides a vital role in balancing the demands and supply of energy, and sometimes the renewable energy must be transported if it did not utilize at the same time. Moreover, the energy generation from the renewables is significantly more when the demand is low, especially under the summer, and that is why the BESS became important. The energy storage plays a vital role in stabilizing energy supply with high shares of intermittent renewable energy sources, and to improve power quality and reliability for grid/microgrid power systems.

1.1 *Background*

The lithium-ion batteries (LIBs) were first commercialized in 1991 and had limited use, colossal size compared to the battery capacity and had a high cost. Today, LIBs are considered high-energy-density batteries and have many advantages over traditional rechargeable batteries, and their development has been very rapid e.g., Reddy et al., (2020). The LIBs provide high energy density, long life, and more safety, and it is also becoming cheaper every year due to technology and development. The batteries have been a promising energy storage technology for emerging applications in automobiles and smart grids (Chen, Zhang, & Amine, 2015).

Nowadays, LIBs are the dominating electrochemical power source in many applications, including electric vehicles and stationary energy storage applications. There are different energy storage technologies, and at the forefront of these technologies are lithium batteries. The high energy density of these lithium batteries makes them very useful for industrial applications. Recently, LIBs storage technology has been installed widely in stationary storage systems with system size range from small (< 20 kWh for residential storage), to medium (< 1 MWh for local applications) and large (> 1 MWh for grid-connected services) (Meng, 2018).

However, LIBs are not perfect technology and need some improvement to be working safely. The main LIBs problem is related to thermal issues. These batteries are susceptible to temperature (Chen, Jiang, Kim, Yang, & Pesaran, 2016). Having a higher or lower temperature than the recommended temperature can lead to problems and thermal impacts in the cell. That can affect the battery lifetime, capacity, operational performance, or in the worst scenario overheating the cell and at which point the cell catches fire, or it explodes. Therefore, a good battery thermal management system (BTMS) is essential. A capable BTMS prevents battery overheating and estimates remaining battery life so that the battery works efficiently and provides stable operating conditions. (You, Bae, Cho, Lee, & Kim, 2018)

1.2 Problem Statement

In the future, more LIBs for energy storage systems are going to be installed. Many of them have been used for the integration of renewable power generation (e.g., PV solar and wind power), and more projects are ongoing and planning, which covers most of the energy storage services in both grid and microgrid applications. Many factors should be taken into consideration regarding the battery system before installation, and they are; safety concerns, cost, life cycle, temperature-related issues. The thermal effects of LIBs and optimized thermal management are critical for safe and reliable operation of LIBs systems. The performance and life span of LIBs are significantly affected by its thermal behavior associated with the cyclic processes and operating temperatures (Ouyang, o.a., 2019). A clear understanding of the thermal properties of LIBs and proper thermal management is essential for system design, ensuring safety, and maintaining good battery performance. This report focused on the commercial LIBs and their BTMS, mainly based on grid/microgrid LIB energy storage application e.g. Vattenfall's LIB energy storage systems and corresponding BTMS.

1.3 Purpose

The purpose of this work is to investigate the status of BTMS technologies applied for stationary lithium-ion BESS and develop a model to study the thermal behavior of the cell. In this study, a model for a battery pack with BTMS using air and liquid cooling was also developed, and the performance of the two cooling systems was compared.

The investigation focused on:

- Status of thermal management technologies applied for stationary lithium-ion BESS with grid/microgrid applications and performing case studies based on industrial applications.
- Developing a battery model and a thermal model for the battery cell to evaluate the thermal performance of LIBs.
- Integrate the battery and thermal model into the battery pack and use it for modeling of BTMS to investigate the thermal behavior of the LIBs system using air and liquid cooling.

1.4 *Research questions*

The following research questions are the focus of this thesis:

- Which existing cooling technologies can be applied for stationary lithium-ion batteries?
- What is the status between air and liquid cooling for the thermal management technologies that can be applied for stationary lithium-ion for grid/microgrid applications?
- What are the most important factors or parameters that affect the major performance of BTMS in specific applications?

1.5 *Delimitation*

The scope of the project is limited for commercial Nickel Manganese Cobalt Oxide (NMC) LIBs applied for the stationary energy storage system due to the time limit and available information. Furthermore, the project further limited to air and liquid cooling system for thermal management of LIBs. The thesis project is based on the battery pack of the BMW car company.

2 METHODOLOGY

This chapter describes the methodology behind this degree project. The project started with a literature study of the status of existing battery thermal management technologies applied for stationary and electrical vehicle (EV) using LIBs. Furthermore, a battery and thermal model were developed to be used for modeling of BTMS.

2.1 Literature review

The literature review was conducted to get more understanding and more profound knowledge about the development of LIBs, their thermal issues, and thermal management technologies. The literature was collected from a reverent search engine, mainly from *Science Direct*, *IEEE Xplore*, and *ResearchGate*. The relevant keywords that have been used in different constellations are *battery models*, *BTMS*, *BESS*, and *electric vehicles*. The literature was reviewed regarding BTMSs available in the market to find a suitable system that can be applied for stationary BESS.

2.2 Battery Thermal modeling

A battery thermal model is developed to investigate the thermal behavior of the LIBs. The equivalent circuit model (ECM) was used for this work and was developed using Simulink in MATLAB. The parameters for ECM were estimated using two experiments, the pulse test, and the low current test. Both experiments were conducted at Vattenfall in a control temperature chamber for three temperatures (0, 25, and 40 °C), and experiment data were provided. The data were used to estimate the ECM parameters. After the parameters were estimated, the thermal model was developed based on the lumped capacitance. Validation of the thermal model against experimental data was then conducted.

2.3 Battery Thermal Management system

The BTMS plays a vital role in the control of battery thermal behavior. The studied BTMS technologies are air and liquid cooling system. These cooling systems are analyzed through a trade-off between performance, reliability, and safety. A model of a specific battery pack was built in Simulink to simulate the thermal behavior of LIBs between the two cooling systems. The pack design and specifications were provided by Vattenfall. The model was later validated using operational data. Finally, case studies were conducted with different battery operating conditions, and the performance of the two cooling systems was simulated and compared.

3 LITERATURE STUDY

In order to identify the status of thermal management technologies applied for industrial applications, a literature review was conducted in this section. This section covers the studies on common LIBs, battery models and thermal battery models, to be used for modeling of BTMS. Furthermore, thermal issues related to the LIBs are studied to clarify the requirement from BTMS.

3.1 Lithium-ion battery

LIBs are an advanced technology that consists of an electrolyte and two electrodes (Figure 1). The negative electrode is called a cathode, and the positive electrode is called an anode where the lithium ions are located when the battery is discharged. The electrolyte consists of a separator, which is the boundary between the anode and cathode, lithium ions move through the electrolyte from positive to negative electrode during the charge. In the positive electrode, the lithium ions carry the electrons, and during the charge, the electrolyte allows only ions to pass through, while the electrons flow through an external circuit, and it is seen as negatively charged. In addition, when the battery is hooked up to power consumption source, electrons flow from negative to positive, and so the battery becomes discharged (University Of Washington, 2020).

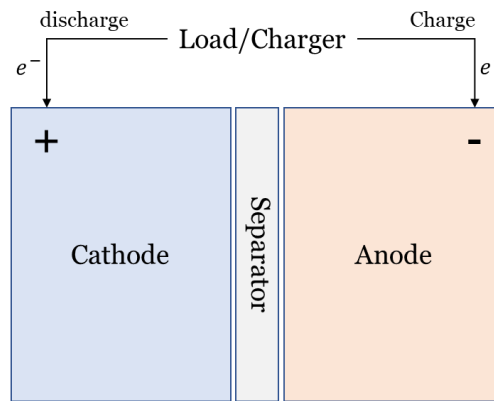


Figure 1 Lithium-ion battery typical component.

The lithium-ion has several cell formats at the market, and the most common ones are the cylindrical, prismatic, and pouch cells. The various cells have different chemistries, designs, and configurations and used for various applications, but the general components that are used in the LIBs battery are similar (Xianxia, Hansan, & Jiujuun, 2011). The lithium cells can be used as primary and secondary batteries. The primary batteries are based on non-electrically reversible chemical reactions that cannot be recharged and generally used for the electronic, while the operation of secondary batteries is based on reversible electrochemical reactions, which makes them rechargeable. The Specific energy of LIBs makes them more suitable for the energy storage systems and other applications such as EV and smaller devices that required consuming power without being connected to a powerline. (Battery university, 2019).

3.1.1 Lithium-ion batteries common chemistries

The Lithium Iron Phosphate (LFP), Lithium Nickel Manganese Cobalt Oxide (NMC), and Lithium Nickel Cobalt Aluminum Oxide (NCA) are the most commonly used cell chemistries. They are all known by their high specific power/energy and high performance. Table 1 and Figure 2 below present the technical differences and similarities of these cell types.

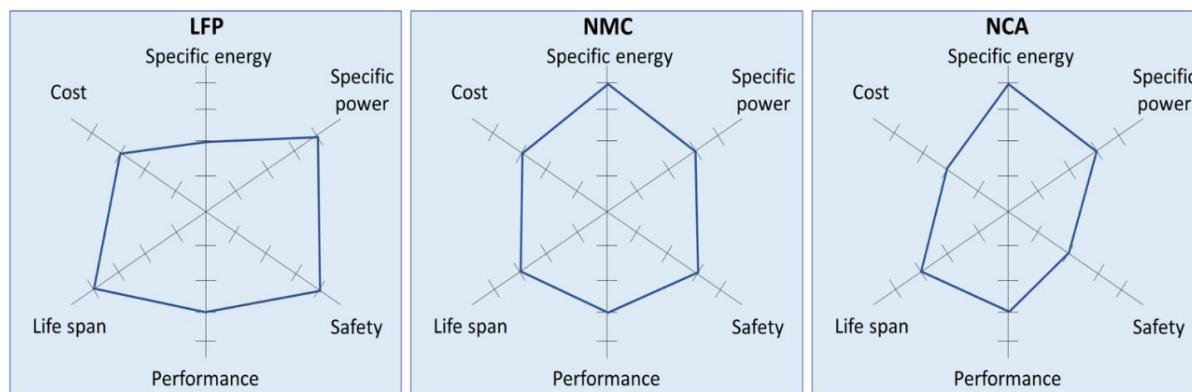


Figure 2 Technical differences and similarities between the most common cell types chemistries. (Battery university, 2019).

Figure 2 shows the comparison of the main performances of LIBs. The general performance mainly depends on battery chemistries and corresponding material properties. The LFP and NMC cell chemistries have safety and specific power capability that gives them the priority of the extensive usage in industrial applications. The NCA shares similarities with NMC by offering high specific energy, reasonably good specific power, and a long life span. The NCA has, on the other hand, less flattering in safety and cost due to the overcharge buffer and the raw material cost of cobalt (Battery university, 2019). More detailed information for the differences and similarities between these lithium-ion chemistries corresponding to Figure 2, presented in Table 1.

Table 1 Properties for the different Lithium-ion cell chemistries. (Battery university, 2019)

Types of Lithium-ion	Lithium Iron Phosphate – LFP	Lithium Nickel Manganese Cobalt Oxide – NMC	Lithium Nickel Cobalt Aluminium Oxide – NCA
Voltages	3.20, 3.30V nominal	3.60V, 3.70V nominal	3.60V nominal
Specific energy (capacity)	90–120Wh/kg	150–220Wh/kg	200–260Wh/kg
Charge (C-rate)	1C typical charges to 3.65V; 3h charge time typical	0.7–1C, charges to 4.20V, some go to 4.30V; 3h charge typical. Charge current above 1C shortens battery life.	0.7C, charges to 4.20V (most cells), 3h charge typical, fast charge possible with some cells
Discharge (C-rate)	1C, 25C on some cells; 40A pulse (2s); 2.50V cut-off (lower than 2V causes damage)	1C; 2C possible on some cells; 2.50V cut-off	1C typical; 3.00V cut- off; high discharge rate shortens battery life
Cycle life	2000	1000–2000	500
Thermal runaway	270°C (518°F) Very safe battery even if fully charged	210°C (410°F) typical. High charge promotes thermal runaway	150°C (302°F) typical, High charge promotes thermal runaway
Cost	~\$580 per kWh	~\$420 per kWh	~\$350 per kWh

Applications	Stationary needing high load currents and endurance	EVs, industrial, Nissan Leaf, Chevy Volt and BMW i3	Industrial, electric powertrain (Tesla)
Temperature range charge	(-20 to 55 °C)	(-0 to 55)	(-0 to 45)
Temperature range dis-charging	(-30 to 55 °C)	(-20 to ~55)	(-20 to 60)
Installed energy 2016 [USD/kWh]	~570	~390	~350
Installed energy 2030 [USD/kWh]	~230	~155	~135

According to Table 1, the Specific Energy is the nominal battery energy per unit mass, sometimes referred to as the gravimetric energy density. Specific energy is a characteristic of the battery chemistry and packaging. Along with the energy consumption of the vehicle, it could determine the battery weight required to achieve a given electric range (Team, 2008).

For the C-rate, it is a measure of the rate at which a cell is charged or discharged relative to its maximum capacity (Team, 2008), and this is described in Equation 1. If a cell is discharged with 1 C-rate, it means that the cell will be discharged in 1 hour, and at a 2 C-rate the cell will be discharged in 0.5 hours or 30 min.

Equation 1 Battery C-rate.

$$C_{rate} (h^{-1}) = \frac{I (A)}{C_{capacity} (Ah)}$$

3.1.2 Key performance of commercial LIBS with different formats

Different lithium-ion cell designs are available on the market due to the variety of users in different projects. The properties for the different lithium-ion cell designs (formats) are classified in Figure 3 below.

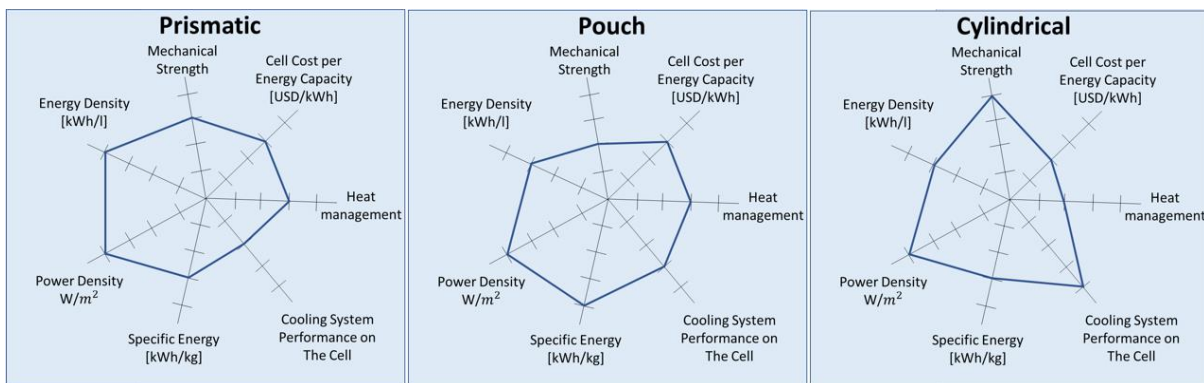





Figure 3 Comparison between different lithium-ion cell designs. (Hannan, Hoque, Hussain, Yusof, & Ker, 2018) (Battery university, 2019) (relionbattery, 2019) (E.Ciez & J.F., 2017) (Miao, Hynan, Von Jouanne, & Yokochi, 2019).

According to Figure 3, the characteristics of Heat management, explaining how the different cell formats can withstand heat. For the Cooling system performance on the cell, it means how efficient to cool down the different cell formats. While the cell cost per energy capacity,

explaining how the cell costs can vary, considering the different cell formats between prismatic, pouch, and cylindrical cells.

Table 2 presents the cell sizes, capacities, and chemistries concerning the most common applications for both EV and energy storage applications. The marked NMC prismatic lithium-ion cell is the one selected to be studied in this project.

Table 2 The most common cell properties concerning industrial applications (Miao, Hynan, Von Jouanne, & Yokochi, 2019), (Battery university, 2019).

Battery (cell)			
	Cylindrical	Pouch	Prismatic
Common sizes	18mm x 65mm	209mm×107mm×8 mm	174mm × 93mm × 23 mm
	21 mm x 70mm	7.25 mm x 160 mm x 227 mm	150mm × 98mm × 28 mm 173mm x 125mm x 45 mm
	26 mm x 65 mm	7.91 mm x 216 mm x 261 mm	173.9mm x 128.1mm x 47.6mm 280mm x 180mm x 69mm
Capacity	1800 – 5000mAh	16 – 50Ah	20 – 120Ah, LFP up to 250Ah
Cell chemistry	(LiNiCoAlO ₂) – NCA (Tesla)	(LiNiMnCoO ₂) – NMC (Nissan Leaf, Chevy)	(LiNiMnCoO ₂) – NMC (LiFePO ₄) – LFP (BMW)

3.1.2.1. Cylindrical cell

The cylindrical cell is one of the most widely used cell types for both primary and secondary packaging styles batteries. The cylindrical cell design has an exterior stainless-steel casing as its package. The battery made by rolling long strips of cathode foil, separator, and anode foil together. The advantage of the cell is the low cost per unit, flexibly to build a system and easy to control the temperature because of the small size and thickness. However, the disadvantage is the small capacity per unit (Lighting Global, 2019).

3.1.2.2. Pouch cell

The pouch cell-like prismatic cell has a thin rectangular form factor. The cell composed of rectangular stacks of individual electrode/separator layers. It uses a laminated flexible aluminum or polymer "bag" as opposed to a rigid metal case as in the prismatic cell. By removing the rigid metal housing, this reduces the cost of the cell, weight, and thickness. However, the cell can have a problem with swelling, which reduces the lifetime, capacity, and make it less safe (Lighting Global, 2019).

3.1.2.3. *Prismatic cell*

The prismatic cell is the one which is known for its high energy content and is similar in construction to cylindrical cells. In prismatic cells, a rectangular aluminum casing is used to reduce the cell's thickness. The electrodes and separator might be rolled similar to the cylindrical cells or can be layered as in a rectangular stack. Some of the applications of the prismatic cell are electric power trains for hybrid and electric vehicles, mobile phones, and tablets (Lighting Global, 2019).

3.2 *Battery models review*

There are a variety of battery models with different objectives and complexity. The models are used to predict the performance of the cell, and to give information on how much heat it can generate. Criteria such as accuracy, number of parameters required for the model, computation time, and complexity must be taken into consideration when choosing a battery model.

3.2.1 *Overview of battery models*

A literature review was done on the various battery models suited for lithium-ion battery; the various models are:

3.2.1.1 *Electrochemical Model*

The model is based on the electrochemical processes that take place in the battery. The aim is to capture all the critical behaviors of the cell and achieve high accuracy. The behavior of the battery's inner cell is simulated using the cell's chemical characteristics and design parameters. The model describes the battery processes in detail. The electrochemical models use complex nonlinear differential equations to describe the battery internal dynamic characters. However, the model often sets up partial differential equations with many unknown parameters. The model is complex and as it uses thermodynamics and electrochemical kinetics equations, which affects its use in real-time applications (Xiaosong, Shengbo, & Huei, 2012).

3.2.1.2 *Stochastic Model*

The focus of the stochastic models is on the recovery effect that is observed when the relaxation times are allowed in between discharges (Panigrahi, o.a., 2001). Furthermore, the models are mainly concerned with the battery recovery characteristics as a Markov process with probabilities in terms of parameters that can be related to the physical characteristics of an electrochemical cell (Zhang, Shang, Duan, & Zhang, 2018). The model is used to estimate battery life in embedded systems applications. The advantage of the model is accurate and can compute faster than the electrochemical model by using partial

differential equations. However, the model is not sufficiently sensitive to predict the experimental data dealing with recovery (Rao, Singhal, Kumar, & Navet, 2005).

3.2.1.3 *Neural network models*

The model consists of three layers, input layer, hidden layer, and output layer. The model's input parameters are SOC and the equivalent circle model parameters, including ohmic resistance, polarization resistance, and capacity (Yanga, Wanga, Pan, Chen, & Chen, 2017). The model has the fastest parallel processing and athletic self-learning ability. However, the model requires a massive amount of data, and the error is susceptible to the training data and methods (Zhang, Shang, Duan, & Zhang, 2018). The model is used to predict the deterioration in battery performance.

3.2.1.4 *Peukert's law model*

The models are mainly used for the lead-acid batteries at constant discharge. It is used to estimate the nonlinear delivered capacity and predict the battery run time of rechargeable lead-acid batteries at different constant discharge current from a fully charged state. However, it does not take into account and ignores the temperature effect on battery nonlinear capacity (Zhang, Shang, Duan, & Zhang, 2018). The models can estimate the battery calendar life for most cases (Jongerden & Haverkort, 2009).

3.2.1.5 *Equivalent Circuit model*

The equivalent circuit model (ECM) is the most common approach for battery numerical analysis (Huria, Ceraolo, Gazzarri, & Jackey, 2012). The model can present the electrical behavior of the battery and can accurately describe the battery I-V characteristics (Zhang, Shang, Duan, & Zhang, 2018). The model considers the influence operational and environmental factors have on the value of the circuit parameters (Aurilio, o.a., 2015). The model can be used for LIBs and as well as other battery chemistries. The EMC is computationally essential and is easy to combine with other methods.

3.2.2 *Summary of battery models*

The models presented in the previous section are summarized in Table 3 to compare their features from:

- Required parameter
- Suitable applications
- Computationally difficulty
- Battery chemistry

Table 3 Battery models summary.

Model type	Required parameter	Suitable applications	Computationally difficulty	Battery chemistry
Electrochemical model	It uses complex nonlinear differential equations and needs to set up partial differential equations with a large number of unknown parameters.	It is used in battery cell design and capture all the critical behaviors of batter cell and achieve high accuracy.	Complicated and long computational time.	All battery chemistries.
Stochastic model	Required experimented data to observe and explore the recovery effect in batteries.	It is used to estimate battery life in embedded systems applications.	The model is fast and reasonably accurate but was found in the literature review to be not sensitive enough to predict the experimental observations.	All battery Chemistries.
Neural network models	It requires a massive amount of data from experiments to train the model.	It is used in battery cell design.	The model has the fastest parallel processing and athletic self-learning ability.	All battery Chemistries.
Peukert's law model	Requires a lot of data from the experiment.	It is used to estimate the nonlinear delivered capacity and predict the battery run time of rechargeable lead-acid batteries at different constant discharge current from a fully charged state.	Easy and straightforward to use with low complexity.	Mainly used for the lead-acid batteries.
Equivalent circuit model	Requires a few parameters, such as: Open circuit voltage, ohmic resistance, current pulse.	It presents the electrical behavior of the battery and can accurately describe the battery I-V characteristics.	The model has low complicity. however, computation time and accuracy dependent on the the number of RC parallel networks.	All battery Chemistries.

3.2.3 Selection of battery model

The model integrations with the BTMS are an essential factor in selecting the suitable model as well as criteria such as accuracy, number of parameters required for the model, computation time, and complexity. Neural network models are fast, but require a considerable amount of data from experiments, which can be hard to find. The Peukert's law model is mainly used for the lead-acid batteries, and the Peukert's law equation does not consider the temperature and cycle life effects on battery capacity. The stochastic model is limited to discharging and requires assumptions to be made in the model and make it not sensitive enough to predict the experimental data. The electrochemical model and equivalent circuit model present a good alternative and can both be integrated with the BTMS. The electrochemical model is the most accurate but for estimating the SOC. However, the electrochemical models are quite complex and involve partial differential equations and to solve in real-time (Gao, Chin, Woo, & Jia,

2017). The equivalent circle model requires a few parameters, gives an accurate result, is suitable for all battery chemistries, suitable for nonlinear conditions, and has low complicity. Therefore, the equivalent circle model is chosen for the battery model in this work.

3.3 Battery thermal models review

There are various thermal models used for battery cells that were found in the literature. The different models have a different impact on the accuracy of the heat transfer in the cell (Damay, Forgez, Bichat, Friedrich, & Ospina, 2013).

The thermal model applied to investigate the temperature profile of the battery cell during the battery's operation. The study by Ahemd A (2002) presents and summarized common models. These models are the following:

- Lumped thermal model
- Partial differential equations (PDEs) models
- Finite element analysis battery model

3.3.1.1 Lumped capacitance thermal model

The model treats the battery core and battery case as two sperate isothermal nodes, all components inside the core such as anode, cathode, active material, etc., are assumed to be a single homogenous material with averaged properties (Ahemd A, 2002). A lumped electric equivalent model is part of the lumped thermal model and is proposed by Damay et al. (2013). The study deals with thermal modeling and experimental validation of a large prismatic Li-ion battery. A one-dimensional lumped thermal model is developed. The heat generated, thermal resistors, and specific heat capacity of the cell is required for the model. The simulation shows that the model is well-suited for applications such as a BMS or off-line applications such as a pack thermal design tool. The simulation tool MATLAB/Simulink can be used to develop such a model.

3.3.1.2 Partial differential equations models

The models contain nonlinear partial differential equations, PDE models can accurately capture system dynamics. The models form complex structure mathematically represented by a series of coupled nonlinear partial differential equations. According to the study by Zou, Manzie, & Nescic (2015), the PDE model is accurate but is a mathematical complex and has long simulation time.

3.3.1.3 Finite element analysis battery thermal model

The model describes the battery heat transfer in three-dimensional. This is presented in the study by Wand, Ma, & Zhang (2017) where a cylindrical Li-ion battery thermal model was

developed using the finite element analysis battery thermal model. The model is accurate and very useful to study how the heat behaves in the cell and surrounding. However, the model requires a massive amount of data, which can be determined through theoretical analysis or experiments, and the simulation time can be too long without powerful computers. The model can be established in the software ANSYS.

3.3.2 Summary of thermal models

The models presented in the previous section are summarized with advantages and disadvantages in Table 4.

Table 4 Battery thermal models summary.

Model type	Advantage	Disadvantage
Lumped capacitance thermal model	It is a simplified and accurate model with low computation time. It can be applied in MATLAB or Simulink. BMS can be integrated into the model.	The model required accurate data for the cell and the surrounding.
Partial differential equations models	Capture the accurately and the system dynamics.	Complex with many nonlinear partial differential equations and have long computation time.
Finite element analysis battery model	It describes the battery heat transfer in a three-dimensional with very accurate model.	A required massive amount of data and have long computation time.

3.3.3 Selection of battery thermal model

The selection of the battery thermal model depends on several criteria such as accuracy, available simulation tools, available data, and integration with BTMS. The PDE model is too complex and requires complicated metastatically equations. The lumped capacitance thermal model is selected in this work. The lumped capacitance thermal model is a simple model that gives good accuracy and fast computation time.

3.4 Main thermal issues and impacts of commercial LIBs

The main thermal issues for LIBs are highly affected by their operation temperature, which could be classified as follows: (Todd M., Srinivas, & Thomas F., 2011)

- Performance degradation at elevated temperatures
- Aging effects at low temperatures
- Thermal runaway under uncontrolled heat generation and abuse conditions
- Temperature maldistribution

3.4.1 Performance degradation

The performance degradation of the lithium-ion cell, explaining how the power loss and capacity fade can occur mainly influenced by the high cell temperature. Besides, the high temperature itself is generated by using high operation conditions like a cell working at a high C-rate. However, the cell performance degradation changes from one cell to another depending upon the different cell chemistries. The capacity fade occurs when the active material inside the battery has been transformed into inactive phases, which reduces capacity at any discharge rate. While the available power is lost when the cell internal impedance increases, which reduces the operating voltage at each discharge rate. All these capacity fade issues have a further impact on cell material and cell aging. Furthermore, the state of charge (SOC) and depth of discharge (DOD) is also a mechanism for cell degradation. This impact of the SOC range can be observed in the remaining studies, according to Todd M., Srinivas, & Thomas F., (2011). For example, K.Takei, o.a., (2001) showed that a cycled C/LiCoO₂ cylindrical batteries in 25% DOD increments, with maximum voltage ranging from 4.27 to 2.78 V. Their results show that the capacity fades increased as the maximum cell voltage increased.

Figure 4 shows a clear summary of the calendar aging, which is highly dependent on the temperature, SOC, and battery chemistries. (Keil, o.a., 2016)

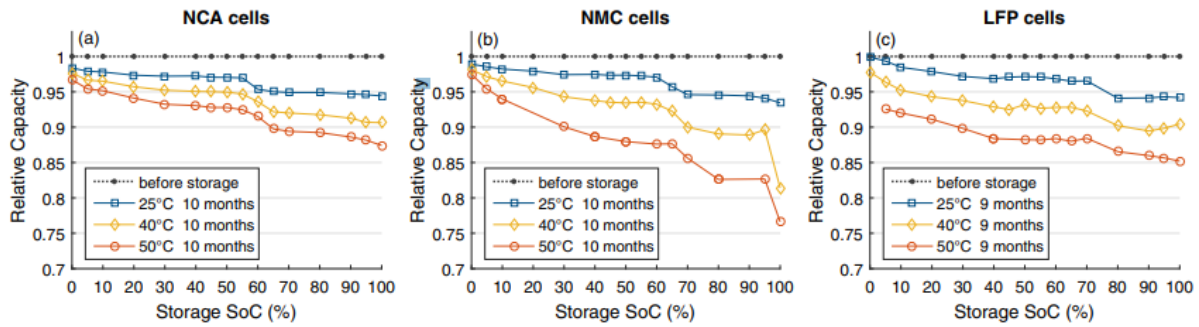


Figure 4 Calendar aging behaviors of three common LIB cells (Schuster, o.a., 2016).

Figure 4 showing comparison between the three common LIB cells NCA, NMC, and LFP after storage of 9-10 months. It is apparent in the figure that the relative capacity of the cells affected by the different storage temperatures and the storage period, which itself led to high DOD. The relative capacity variety between the three different cells in Figure 4 depends on the different cell chemistries and can explain which cell can withstand high DOD more than others. (Schuster, o.a., 2016). Considering the massive combinations of diverse electrode materials and electrolyte composites, it's impractical to cover the performance degradation mechanisms of all these electrochemical batteries. However, according to Ning, Haran, & N.Popov, (2003), the capacity fade is attributed to lithium loss and active material reduction inside the battery, while the origin of power abatement is the increasing cell internal resistance due to the elevated temperature according to R.Belt, D.Ho, G.Motloch, J.Miller, & Q.Duong (2003).

3.4.2 Low-temperature effects

It has been indicated that the high cell temperature leads to performance degradation of LIBs. Many studies have implied that the cell performance is also reduced under low temperature,

and it is another main thermal issue. A low cell temperature could be affected by the ambient temperature, mostly in a condition such for example, when a failure occurs in the battery heating system in cold ambient temperature. However, the exact mechanisms leading to the poor performance of LIBs at cold temperatures are still under debate and needs to be studied further (Huaqiang, 2017). Nonetheless, the performance of LIBs is reduced at lower temperatures for all cell materials. In addition, the charge performance is substantially less than that for discharge. It can be seen that the battery capacity drops with temperature, especially below -20°C . Although the ionic conductivity of the solid electrolyte interphase (SEI) and electrolyte and the diffusion of lithium into the graphite can be reduced significantly at low temperatures, (Zhang, Xu, & Jow, T., 2003) argue that poor performance of LIBs at low temperatures is linked to poor charge transfer at the electrode/electrolyte interface. In fact, this poor charge transfer can lead to substantial plating on the negative electrode during charging, which can cause irreversible capacity loss from electrolyte reduction (Todd M., Srinivas, & Thomas F., 2011). A further consequence at low temperatures could also result in a localized degradation to short battery lifetime, especially during charging. It means that the charge performance degrades more quickly than discharge performance under cold conditions (Wiebelt, 2018).

3.4.3 Thermal Runaway

Thermal failure of individual lithium-ion cells could be initiated for different reasons, most likely in situations such as internal short-circuit, overheating, and overcharging or discharging. These reasons further cause an initial increase in cell temperature and trigger chemical reactions. The highly exothermic reactions result in a rapid self-heating of the cell, i.e., thermal runaway (TR) (Xuning, Mou, Xiangming, & languang, 2014).

The TR is used to evaluate the safety of different batteries with different materials under the same testing conditions. Moreover, TR describes a situation when a battery cell spontaneously self-destructs due to temperature increases, which is often resulted by an internal short circuit and undergoes two events in sequence, i.e., heat-generating resulted in hot spots and triggering the propagation of anode that would dramatically increase the temperature of the cell (Zhengming John, Premanand, & Weifeng, 2014).

When the cell is overheated, it means the cell temperature is rising above a certain limit. The reason behind that is when, for example, a failure occurs in BTMS, and the battery generated heat could not be removed. In addition, that will further increase the temperature inside the cell and ends with a severe exothermic reaction that comes one after another, called thermal runaway. The same thing will happen when a short circuit occurs. A short circuit leads to uncontrollable heat generation inside the cell. What happens is that the positive terminal of a battery somehow gets direct into contact with the negative terminal of the cell. This is how LIBs can lead to fires in extreme cases. (Yang, o.a., 2019)

The thermal runaway is initiated at a different cell temperature, and that depending on the cell's SEI layer decomposition. SEI is the protective layer between the positive and negative electrodes. For example, the cell type LFP has the SEI layer decomposition at 100°C , that is when the SEI starts to damage, and a reaction occurs between the electrolyte and electrode.

The SEI starts melting at 143°C, which further causes an internal short circuit. A thermal runaway takes place when the temperature starts increasing over 150°C. (Yang, o.a., 2019)

3.4.4 *Temperature distribution*

For better cell performance, the temperature distribution inside the cell should be as uninformed as possible. If the heat is not transferred properly, the cell can be damaged or at least will harm its performance, safety, and lifetime. Prevents these problems, temperature distribution depends strongly on the BTMS and mainly on the properties of the coolant and the design of the flow channels of the battery pack. Besides, a basic cooling system for BTMS, like passive air cooling, will have uneven temperature distribution inside the battery pack. That is because the heat transfer is higher at the outer surface of the battery pack, and the temperature maldistribution will lead to capacity variability between the cells in the pack. This then will create a vicious cycle, which means the cells with proper temperature need to deliver higher power to compensate for the low performing cells. Furthermore, the cells that deliver higher power will lead to an increase in its actual temperature. Therefore, severe temperature maldistribution should be avoided, and the maximum temperature deviation inside the battery pack is usually expected to be below 5 °C. (Guodong, Lei, & Guanglong, 2017)

3.5 *Handling thermal issues and impacts of commercial LIBs*

As mentioned in the previous sections, the temperature and operation conditions of the battery have a significant impact on the performance, lifetime, and safety of the batteries. BTMSs/processes ensure the battery energy storage systems to be operated in a suitable temperature range and avoid the safety risks. (Chen, Jiang, Kim, Yang, & Pesaran, 2016) . Therefore, BTMSs must be included for every battery system. There are two main functions of BTM processes described by Yang, o.a., (2019).

- Keep batteries working under a suitable temperature range and uniform temperature distribution to improve the electrical performance and battery life span.
- Prevent thermal failures and thermal runaway to improve safety.

Figure 5 shows the nominal operating conditions for LIBs. The operating conditions show an optimum temperature range for LIBs is between 15 - 35 °C and the maximum temperature difference in the cell should not exceed 5 degrees. According to Figure 5, the operation conditions out of this range, the battery will not work correctly, results in poor performance, or even damaging or thermal runaway, and therefore requires either heating or cooling.

Operating temperature	−20 °C	0 °C	20 °C	40 °C	60 °C
Power and availability	< 70 % Very high R_{zi}	90 % High R_{zi}	100 %	100 % → 0 % Throttling	
Service life	Cell aging During charging		Optimum temperature	Cell aging/ → Thermal runaway	
Thermal management	Heating				Cooling
	$\Delta T_{Cell} < 5 K$				

Figure 5 Nominal operation condition for the lithium-ion cells (Wiebelt, 2018).

Other factors are also affected by battery temperatures, such as battery aging, cycles, and power content. The R_{zi} is a variable that is describing the resistance of the electrical power inside the cell. As much the operation temperature is under the limit, the useful power availability in the cell will decrease. This can also be explained as performance degradation, which caused by low-temperature effects (Wiebelt, 2018).

For avoiding performance degradation and calendar aging, there are some requirements for the storage of LIBs that could be applied, and they are, according to Huaqiang (2017) as follows:

- The storing environment should be dry and clean with adequate ventilation and desired ambient temperature
- The direct exposure to sunlight should be avoided
- The distance from the battery to any heat source should be at least 2 meters
- Being placed upside down or any mechanical stress is not recommended

BTMS becomes more vital and efficient when it comes to battery packs design, especially for air cooling. The battery pack design still as crucial as BTMS. It is shown that the BTMS improved through designing the flow pattern of the air-cooling system (Kai, Weixiong, Fang, Lin, & Shuangfeng, 2019). Even if there is a high-performance thermal management system (TMS) for commercial LIBs, the pack design can have a reason behind the mentioned thermal issues in the previous section. The main going researches for LIBs electrical performance, life span, and safety are to find an efficient combination between the cells' design inside a pack/module and BTMS.

3.6 Cooling systems applied for LIBs

In some applications, the LIBs used for strange conditions where the charging and discharging current is high powered. In this kind of application, the battery heat generation rates are excessive and lead to an increase in the battery operating temperature. These can increase battery frailty and safety hazards. Therefore, there are different cooling systems used for the BTMS for high powered applications such as EV and BESS (Sayed Saeed, Maciej Jozef, &

Søren, 2017). In this report, various BTMS have been studied for a range of lithium-ion battery geometries and operating conditions. Besides, further BTMS has been proposed to be used for Vattenfall future battery energy storage applications.

The main categories of BTMS that have been studied are the air-based and liquid-based cooling systems. These cooling systems are mostly used in the industrial applications in both EV and BESS. Figure 6 shows the two main BTMS based on the cooling medium: air and liquid (Zhonghao & Shuangfeng, 2011).

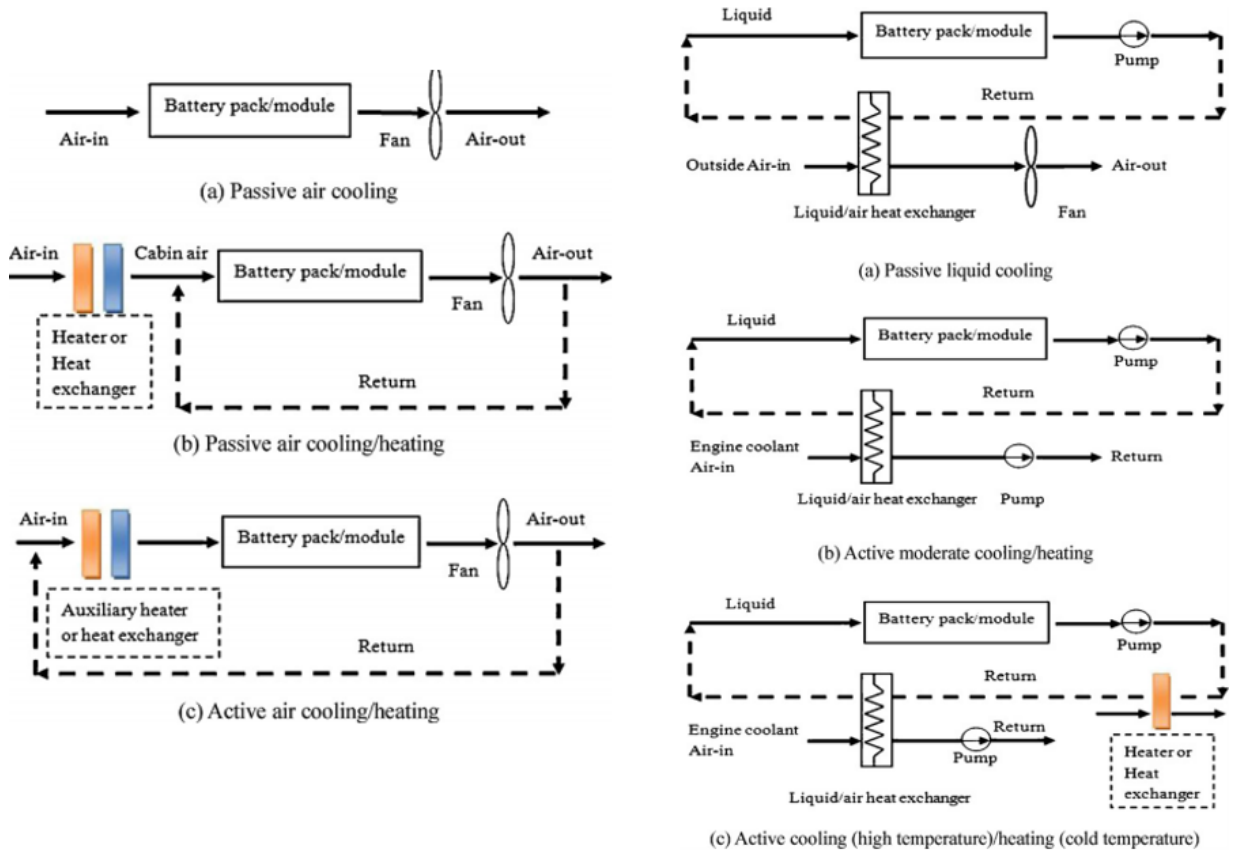


Figure 6 Thermal management using air cooling (left) and liquid cooling (right) (Zhonghao & Shuangfeng, 2011).

3.6.1 Air cooling

For the air-based BTMS, there are two main categories, according to Figure 6: natural airflow convection and forced airflow convection. It is also known for passive and active air cooling. For the forced (active) air cooling, the airflow is forced into the battery pack to enhance heat transfer using an energy-consuming source such as a high-powered fan/blower. While for the natural (passive) air cooling, the air convection flows into the battery pack that occurs without consuming notice energy, which is only suitable for low-density batteries. The only advantage when using passive air cooling is the lower financial cost compared to the active air cooling. (Maan, Ibrahim, & Marc A, 2018)

For the LIBs used in industrial applications, most of the proposed air-based BTMS are forced (Active) air convection systems, according to Table 5. This is because the forced air cooling has

a higher heat transfer coefficient than natural air cooling. Furthermore, LIBs that are used in industrial applications work under strange conditions, which means that the batteries work at high charge/discharge rate and require a more efficient cooling system to prevent any frailty and safety hazards. That does not mean that the forced air cooling is best for BTMS in the industrial application, but it is proposed mainly for battery packs subject to moderate cooling loads.

There are three main variables for the air-cooling system. These variables can improve or decrease the efficiency of the system, and they are (1) airflow velocities, (2) flow path, and (3) geometrical arrangement of the batteries in the pack (Maan, Ibrahim, & Marc A, 2018). A summary of the main studied air-based BTMS for LIBs used for industrial applications is presented in Table 5 below.

Table 5 Summary of the air-cooling system used in industrial applications for BTMS.

Industrial applications	Cell Type & size (mm)	Cooling system	Nominal C-Rates	Number of cells in Pack	Pack energy content (kWh)	Cell capacity (Ah)	References
Nissan Leaf EV	Pouch NMC 7.91 x 216 x 261	Passive (Air cooling)	1/3C – 1C	192	24	33	(qnovo, 2015)
BYD BESS	Prismatic LFP 58 x 145 x 415	AC active (Air cooling)	—	16	12.8	230	(Gatta, o.a., 2016), (safecloudenergy, 2018), (Torre, 2015), (Battery)
Samsung SDI Mega M2-P2 BESS	Prismatic NMC 174 x 93 x 23 - 173 x 125 x 45	HVAC active (Air cooling)	1C – 2.5C	22	6 – 8	68 – 94 – 111	(Samsung, 2018) (Samsung, 2017)
HITACHI BESS	Cylindrical CH75-6	Forced (Air cooling)	1C – 2.2C	6	1.665	75	(Hirota, Hara, Ochida, & Mishiro, 2015)
TESVOLT BESS	Prismatic NMC 173 x 125 x 45	HVAC (Air cooling)	1C	14	4.87	94	(Tesvolt, 2018)
Integrated BMW BESS	Prismatic NMC 173 x 125 x 45	AC active (Air cooling)	0.3C	96	33.2	94	Vattenfall, 2019. A vehicle lithium-ion battery system BMW
JRC's Smart Grid BESS	Prismatic NMC 148 x 98 x 27	HVAC active (Air cooling)	~ 0.4C	16	3.97	68	(Rancilio, o.a., 2019)

According to Table 5, the air-cooling system has been widely used on BESS. The air cooling might not be a preferred cooling system due to it is low heat capacity and low thermal conductivity. However, it is still an attractive solution for BTMS because there is no leaks potential and no heat exchangers. It is also less complicated and more comfortable to maintain compared to liquid cooling. The only cooling system in Table 5 that is based on passive air

convection is for Nissan Leaf EV. The movement of the car during drive gives the battery pack an advantage of airflow through it and making the passive cooling system more efficient.

3.6.2 *Liquid cooling*

Same as for air cooling, the liquid-based BTMS consists of two main categories, according to Figure 6: passive and active liquid cooling. For the active liquid cooling, there are two loops, which are the primary loop and the secondary loop. The primary loop is the same as the loop in a passive liquid system, where the heat transfer fluid is circulated by a pump. The secondary loop can be an air conditioning loop. The upper heat exchanger, instead of being a radiator, works as an evaporator for cooling operation and connects both loops. While for the passive liquid cooling, the heat-sink for cooling is a radiator. Heat transfer fluid is circulated by the pump in a closed system. The circulating fluid absorbs heat from the battery pack and releases heat through a cooler. The cooling power depends strongly on the temperature between the ambient air and the battery. The fans behind the radiator can improve cooling performance, but if the ambient air is higher than the battery temperature or the difference between them is too small, the passive liquid system becomes ineffective. (Zhonghao & Shuangfeng, 2011)

The liquid coolant has more advantages compared to air. The advantages of using liquid coolant are that it can handle large cooling loads in scenarios such as defects in cells, high power draws, and high environmental temperatures. The main disadvantage when using liquid cooling is that it is complex, has leakage potential and such a high cost. (Guodong, Lei, & Guanglong, 2017)

The liquid cooling for BTMS, according to the summary in Table 6, has mostly used in EV applications. The advantage of using liquid cooling in EV is that it is more compact and makes the battery pack consuming fewer spaces in the EV compared to the air-cooling system. In addition, due to the liquid coolant high thermal conductivity and high heat transfer coefficient, the major EV manufacturers using liquid cooling systems to maintain their batteries within the optimum operating range. (Maan, Ibrahim, & Marc A, 2018)

There are four main variables for the liquid -cooling system. Same as for the air cooling, these variables can improve or decrease the efficiency of the system, and they are (1) number of channels, (2) inlet mass flow rate, (3) flow direction, and (4) width of channels. (Qian, Li, & Rao, 2016)

Table 6 Summary of the liquid-cooling system used in industrial applications for BTMS.

Industrial applications	Cell Type & size (mm)	Cooling system	Nominal C-rate	Number of cells in Pack	Pack energy content (kWh)	Cell capacity (Ah)	References
BMW i3 EV	Prismatic NMC 173 x 125 x 45	Refrigerant cold plate active (liquid cooling)	1.2	96	33.2	94	Vattenfall, 2019. A vehicle lithium-ion battery system BMW
Tesla S model EV	Cylindrical 18650-format NCA	Glycol tubs active (liquid cooling)	1C-2C	7104	85	3.3	(Field, 2019)
Chevrolet EV	Pouch NMC 6.3 x 127 x 177	cold plate active (liquid cooling)	1.5C -	192	18.4	25.2	(VOLT, 2016), (Arcus, 2016)
Integrated BMW SE09 BESS	Prismatic NMC 173.9 x 128.1 x 47.6	Refrigerant active (liquid cooling)	1.2	96	42	120	Vattenfall, 2019. A vehicle lithium-ion battery system BMW
Integrated Tesla model s BESS	Cylindrical 18650-format NCA	Glycol tubs active (liquid cooling)	~ 0.6	600	6.5	3.3	(Tesla, u.d.)

The liquid cooling can also be classified as direct and indirect cooling. Due to the cost and safety concerns, such as the short-circuit and leakage potential, the direct liquid cooling system for BTMS might not be the desired solution for most of the current applications. However, the direct liquid cooling should be dielectric with low viscosity and high thermal conductivity and thermal capacity compared to the indirect system.

3.6.3 Comparison between air and liquid cooling system

The specifications and key performance indicators (KPI) for both air and liquid cooling systems were studied. The general comparison between these cooling systems that are used for the LIBs for industrial applications was presented in Figure 7. When it comes to complexity, the liquid cooling system is more complicated due to its weight, constructions, maintenance, and space requirements. Furthermore, the addition of heat exchangers and circuits for the system makes liquid cooling more expensive than air cooling.

The liquid cooling is also riskier to use than air cooling due to its leakage potential that could result in a short circuit. As mentioned before, a short circuit could occur when the positive terminal of a battery somehow gets direct into contact with the negative terminal. In this case, the liquid could be the reason for the contact between the positive and negative terminal, which itself has excellent electrical conductivity. However, using air cooling for a lithium-ion cell that works at high charge/discharge rate is also risky, and can result in unwanted real consequences such as thermal runaway, as mentioned before.

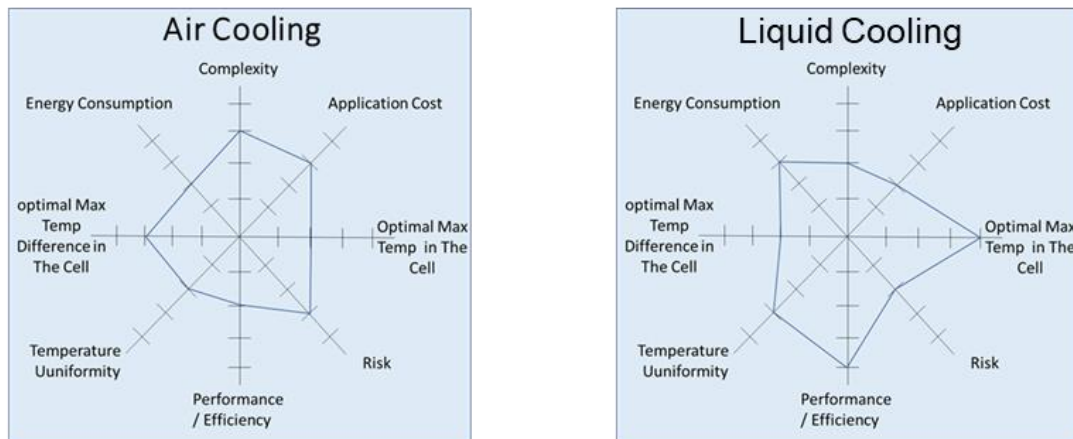


Figure 7 General KPI for both air and liquid cooling systems. (Chen, Jiang, Kim, Yang, & Pesaran, 2016), (Kim, Ho, Marina, & Eugene, 2012), (Han, Khalighi, & Kaushik, 2017), (Khan, Nielsen, & Kær, 2014), (Madani, Swierczynski, & Kær, 2017).

Even though liquid cooling has some disadvantages that are mentioned above, it still has better performance than air cooling. When it comes to thermal conductivity, heat capacity, and precise control for heating/cooling, liquid cooling is more efficient (Han, Khalighi, & Kaushik, 2017). This improves the more uniform cell temperature distribution and keeps the optimal max temperature under the limit of the lithium-ion cell avoiding cell aging, decreasing cycles, and decreasing power content. The summary of the differences between both air and liquid cooling systems were studied for LIBs. Table 7 shown the advantages and disadvantages of the liquid cooling systems of commercial LIBs.

Table 7 Advantages and disadvantages of the liquid cooling systems. (Maan, Ibrahim, & Marc A, 2018), (S.Panchal, o.a., 2017), (Qian, Li, & Rao, 2016), (E, o.a., 2018),

Liquid cooling	
Advantages	Disadvantages
<p>It can be 3500 times more effective than air cooling due to itis has high thermal conductivity and high heat transfer coefficient with the ability to absorb more heat, compared with air cooling, and it occupies less volume.</p> <p>It handles large cooling loads in scenarios (high power draws, high environment temperatures).</p> <p>Ability to decrease energy consumption by constructing a wider cooling channel, and that leads to a lower pressure drop. The pressure drop can go up to 55 % when the channel broad changes from 3 mm to 6 mm.</p> <p>Better thermal balance and uniformity could be achieved using liquid cooling.</p>	<p>The liquid cooling system is more complicated compared to air cooling due to the addition of heat exchangers and circuits.</p> <p>Higher cost compared to air cooling.</p> <p>Higher specific weighs of the cooling system, the high coolant weight, due to the high density of the liquid.</p> <p>The increase in coolant velocity corresponds to an increase in energy consumption.</p> <p>Requires more often maintenance than air cooling</p> <p>Potential leakage that can make manufacturers hesitate to use liquid cooling for the lithium-ion cells.</p> <p>Increase temperature difference in the cell.</p>

While Table 8 shown the advantages and disadvantages of the air-cooling systems of commercial LIBs.

Table 8 Advantages and disadvantages of the air-cooling systems. (Lip, o.a., 2016), (Zhoujian, Li, Yong, Chao, & Xuejiao, 2017), (Chen, Jiang, Kim, Yang, & Pesaran, 2016), (Chen, Jiang, Kim, Yang, & Pesaran, 2016).

Air cooling	
Advantages	Disadvantages
<p>The air cooling is consuming smaller space within the electric vehicle because the coolant is not recycled again.</p> <p>It can be passive systems in which air flows through the battery pack due to the movement of the EV.</p> <p>Simple structure, easy maintenance, low cost, and parasitic energy consumption is low during the system operation process due to the lower air viscosity.</p> <p>The cylindrical batteries achieve better performance from air cooling, since the investigated parametric influence on a cylindrical battery module due to the battery's distribution and size compared with prismatic batteries</p> <p>For the prismatic cell, in some cases, such as parallel hybrid electrical vehicles (HEVs), air cooling is adequate.</p> <p>For prismatic cells, an air-cooling system works very well in HEVs during standard drive cycles that could control the maximum temperature below the limit of 55 °C and the temperature difference, not more than 5 °C in the cell.</p>	<p>The low heat capacity of air leads to a thermal gradient through the battery pack.</p> <p>The low heat capacity of air and the nature of cooling through sensible heat, resulting in a limited ability of cooling, and it also imposes some constraints on the location of the battery pack.</p> <p>Heat load is limited to about 325–800 W, depending on vehicle cabin air temperature.</p> <p>When the battery pack scale is large, the system requires a high power output, and the ambient temperature is too high or too low, the air cooling system may not meet the requirement of thermal management.</p> <p>Using prismatic battery during aggressive driving circles and at high operating temperatures, it will inevitably cause a large nonuniform distribution of temperature in the battery.</p> <p>The maximum temperature can be higher than the desired limit on an aggressive cycle.</p>

4 CASE STUDIES

The case studies for this work conducted with the following sections:

- Battery Model (ECM)
- Battery Thermal Model
- BTMS

The work started with developing a model that can predict the temperature in the LIBs involves the combination of different models. These models also involve various steps for each, and in the end, they are combined to achieve the desired goal. In the beginning, the equivalent circuit model ECM was selected. The ECM model implies that the initial model parameters, such as the resistances, capacitances, and OCV with SOC relationship, must be first determined. When the initial model parameters were estimated for the equivalent circuit model, it was then combined with heat generation and thermal sub-models in the MATLAB-Simulink. Finally, when a battery model (ECM) and thermal model were developed. The model was validated against experimental data to ensure the accuracy of the model. The cell model was integrated to pack size and was developed based on the thermal model of the cell. The BTMS for the pack is used to control the battery's thermal behavior. The pack model was validated against operational data from existing BESS. Finally, in the simulations, the BTMS system was used further to analyze different cell operation conditions to identify the operating limitations of the pack using air or liquid cooling. The result can be found in the result section.

The cell that is used in this work is 120 Ah capacity with NMC chemistry. The cell has a large capacity and used in both EV and commercial stationary applications. The cell technical specifications are presented in Table 9.

Table 9 General technical specifications of the cell

Battery Cell Type	Prismatic
Nominal capacity	120 Ah
Nominal voltage	3.68 V
Energy content	439 Wh
Dimensions	174 × 128 × 48 mm
Cell chemistry	NMC

4.1 Battery Model

The ECM is the most common model for LIBs and describes the internal electrochemical reaction in a conventional two-terminal battery. Among the equivalent circuit models, the Thevenin equivalent circuit model is used in this study. The ECM model is presented in Figure 8 and is based on work by Huria et al. (2012).

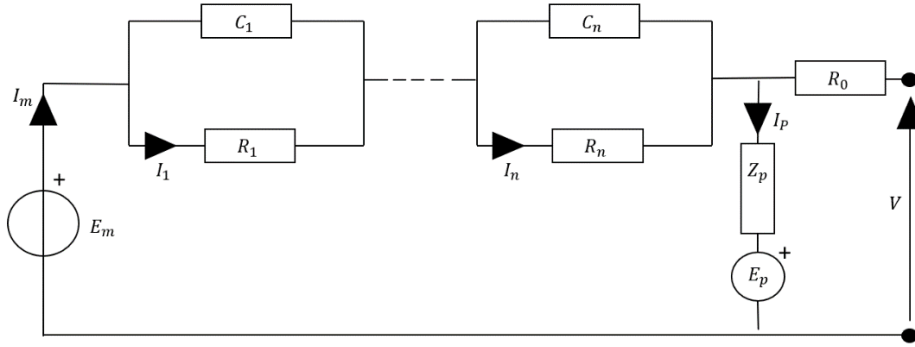


Figure 8 General equivalent circuit model.

A general equivalent circuit model with an n-RC network for a LIB is shown in Figure 8. The description of the symbols is presented in Table 10. The parameters are functions of battery SOC, Temperature, and tend to be nonlinear.

Table 10 Symbols description of ECM of the cell.

Symbol	Description	Unit
C_n	Polarization capacitance	F
E_m	Electromotive force	V
E_p	The electromotive force of parasitic branch	V
I_m	Current in the main branch	A
I_p	Current in the parasitic branch	A
n	Natural number	-
OCV	Open-circuit voltage	V
R_o	Internal resistance	Ω
R_n	Polarization resistance	Ω
Z_p	Impedance of parasitic branch	Ω

The choice of several RC parallel networks (resistor-capacitor) is a trade-off between the relevant experimental data and equivalent circuit complexity. The difference using one or three RC networks is described in the study conducted by You, Bae, Cho, Lee, & Kim (2018). The study compares the accuracy of having one or three RC parallel networks. Three RC parallel networks give higher accuracy. However, it is more complex, and the computation time is longer. According to Low Wen et al. (2013), with two RC parallel networks, the model still has high accuracy with fast computation time. Therefore, the battery model with two RC parallel networks is applied in this work. The parasitic branch can be neglected for cell if it has high coulombic efficiencies (CE), according to Huria et al. (2012). The CE is defined as the total discharge capacity and charge capacity (Equation 2).

Equation 2 Coulombic efficiencies.

$$\eta_{Coulombic} = \frac{Capacity_{discharge}}{Capacity_{charge}}$$

The CE was estimated at Vattenfall for the cell. The result shows that the CE is over 98%, and the parasitic branch can be neglected. The simplified ECM used in this work is presented in Figure 9.

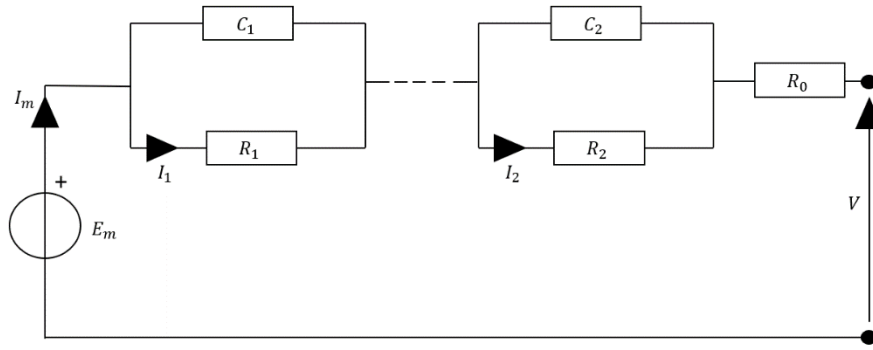


Figure 9 Simplified ECM for lithium-ion batteries with two RC parallel networks and neglect of the parasitic branch.

The main parameters for two RC blocks ECM are R_o , R_1 , R_2 , C_1 , C_2 , and E_m (i.e., open-circuit voltage OCV), which are functions of SOC and temperature. These parameters can be estimated by conducting a pulse test and a low current experiment.

Coulomb-counting is used to estimate SOC and is described in Equation 3. t_0 represents the initial state, and C_N represents rated stored battery capacity. The OCV is estimated in Equation 4. Terminal voltage is the measured voltage from the cells two terminals using a multimeter. Internal voltage can be estimated from Ohm's law (Equation 5), and the voltage of the RC parallel network is estimated by Kirchhoff's current law in Equation 6.

Equation 3 Coulomb counting.

$$SOC(t) = SOC(t_0) + \frac{1}{C_N} \int_{t_0}^t I(t) dt$$

Equation 5 Ohm's law.

$$V = I * R$$

Equation 4 Calculate OCV.

$$OCV = V_{terminal} + V_1 + V_2 + V_0$$

Equation 6 Kirchhoff's current law.

$$C \frac{dV}{dt} + \frac{V}{R} = 0$$

4.1.1 Parameter Identification

The accuracy of the ECM is dependent on the parameters in the model. The parameters identified using measurement data obtained from the pulse test and low current experiment. This section covers the approach used for the parameter identifications.

The approach in this work follows the same methodology used in the study by Huria et al. (2012). Furthermore, as stated earlier, two RC parallel networks are used. The methodology is illustrated in the flow diagram and is illustrated in Figure 10.

The pulse test experiment was done for three temperatures (0, 25, and 40 °C). The current profile for charge and discharge was taken from the test and used in the model to get the terminal voltage. The simulated voltage later compared with the measured voltage from the pulse test experiment. If the simulated voltage does not match the measured voltage, the parameters (E_m , R_0 , R_1 , R_2 , C_1 , C_2) were modified until the two voltage matches. The function "parameter estimation" in Simulink was used to modify the parameters. Here it is vital to have an understanding of the range, the maximum and minimum values. The main objective is to match the voltage profile of the pulse test with simulation voltage.

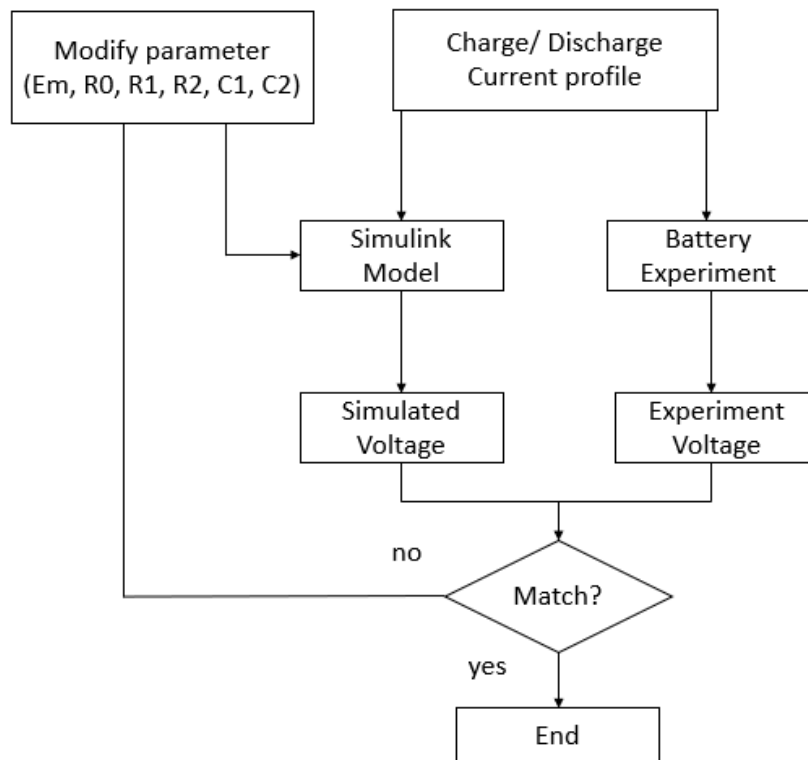


Figure 10 Flow diagram of parameter estimation.

4.1.2 Parameter estimation

From the pulse test, R_0 , R_1 , R_2 , C_1 , and C_2 can be obtained for the ECM. The data correlation is illustrated in Figure 11, where SOC and OCV are measured under the rest period, where there is no current, and the voltage is in steady-state. The R_0 affects the instantaneous response, and the RC parallel networks affect the delayed response.

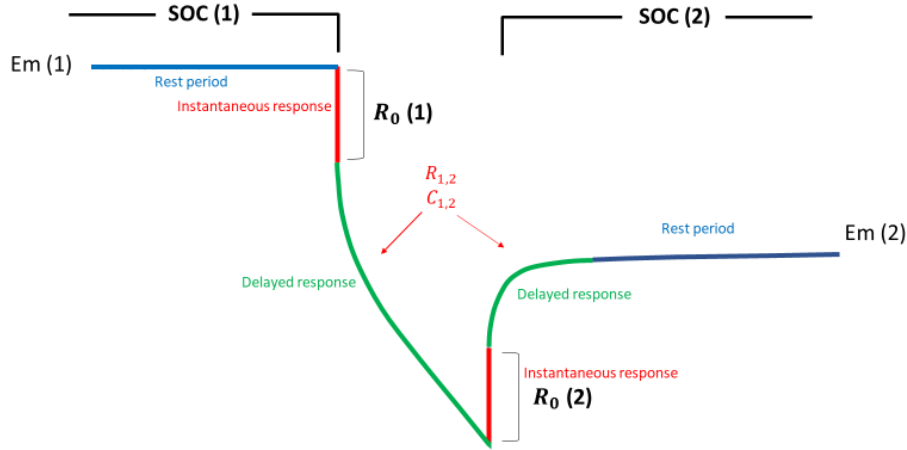


Figure 11 Data correlation to the ECM.

The voltage measured from the low current test represents the OCV. There are low voltage losses from the resistance when using low C-rate, and the voltages (V_0 , V_1 , and V_2) are negligible in Equation 4, and the terminal voltage can be assumed to be the OCV. All the parameters for the three different temperatures for charge and discharge were estimated for the cell for various SOC. However, the parameters are considered as confidential information for Vattenfall and will not be disclosed in this work.

4.1.3 Experiments

In order to identify the parameters, two tests were performed, the pulse test and low current experiment. The experiments were performed for the battery cell for three temperatures (0, 25, and 40 °C) by having the cell in a controlled temperature chamber. Both experiments were performed at Vattenfall Intertek, and later the test results were provided.

4.1.3.1 Pulse test

The characterization of constant current pulse discharge/charge experiment was carried out with the following procedure:

- Step 1: The battery is fully discharged/charged and kept at a constant temperature.
- Step 2: The battery cell is subject to pulse constant at 60 A current for a short time.

- Step 3: After the battery is charge/discharge with a short pulse current, the cell is allowed to rest for a longer time. This is to get the OCV at a steady state for higher accuracy and keep the temperature controlled.
- Step 4: Repeat steps 2 and 3 in a number of cycles depending on the battery capacity.
- Step 5: The experiment is repeated for different temperatures.

An example of the pulse test measurand data is illustrated in Figure 12. The data is for one battery cell with discharge pulse 60 A with temperature in the cell kept constant around 40°C.

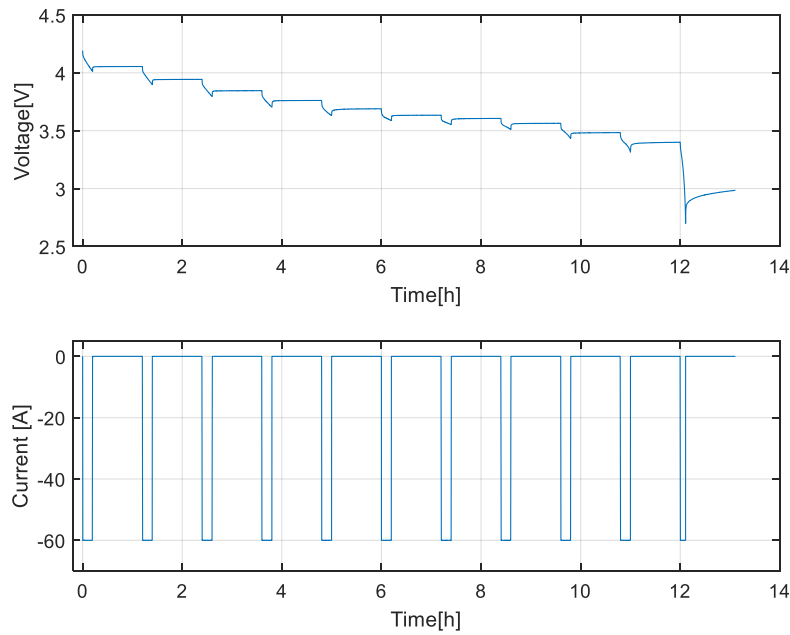


Figure 12 Measured data from pulse test for 40°C discharge.

4.1.3.2 Low current experiment

The low current experiment was conducted for the battery cell. The purpose is to estimate the OCV accurately. The characterization of low current discharge/charge experiment was carried out with the following procedure:

- Step 1: The battery is fully discharged/charged and kept at a constant temperature.
- Step 2: The battery cell is subject to constant low current around for a long time, depending on the battery capacity. The experiment is conducted with the low current to reduce losses and thus reduces errors.
- Step 3: The experiment is repeated for different temperatures.

An example of the low current experiment measurand data is illustrated in Figure 13. The data is for one battery cell with a discharge pulse of 2.4 A or 0.02 C-rate with temperature in the cell around 40°C.

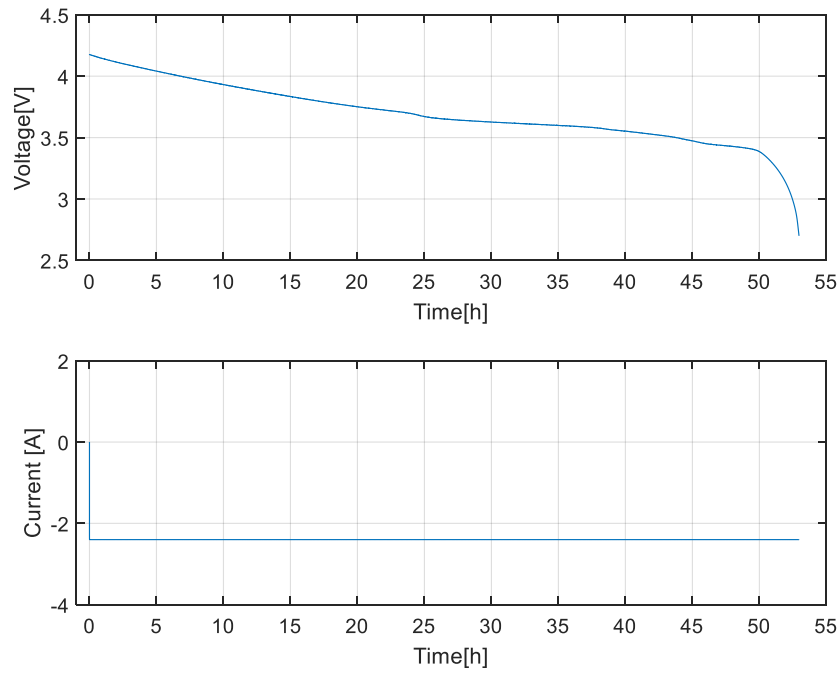


Figure 13 Measured data from low current experiment for 40°C discharge.

The estimated OCV curves for the charge and discharge for the three temperatures can be found in Appendix 1. The OCV initial and end voltage for charge and discharge for the three temperatures is presented in Table 11.

Table 11 OCV Initial and End.

Charge		
Temperature (°C)	Initial (V)	End (V)
0	2.88	4.2
25	2.92	4.2
40	2.86	4.2
Discharge		
Temperature (°C)	Initial (V)	End (V)
0	4.181	2.5
25	4.188	2.7
40	4.179	2.7

4.2 Battery Thermal Model

The thermal model is developed using the electrical parameters for the ECM. The cell heat generation and heat transfer are developed in a model and later validated against experimental data.

4.2.1 Heat generation in Lithium-ion Batteries

Energy conversion through chemical, electrical, and mass transport processes is responsible for the heat generated during the operation of the battery cell. Reliable predictions of cell temperature and heat generation rate are required for the developing thermal model. The two main heat sources in the cell are the irreversible and reversible heat (Damay, Forgez, Bichat, Friedrich, & Ospina, 2013) and can be described in Equation 7.

Equation 7 Heat generation.

$$\dot{Q}_{gen} = \dot{Q}_{irr} + \dot{Q}_{rev}$$

The irreversible heat, also called the joule effect are ohmic losses in the cell from the electrical resistances (Makinejad, o.a., 2015). This is presented in Equation 8.

Equation 8 Irreversible heat.

$$\dot{Q}_{irr} = I_{cell} * (V_{cell} - V_{OCV}) = I_{cell}^2 (R_0 + R_1 + R_2)$$

The reversible heat mechanism consists of the entropy effect, and heat is generated or consumed because of the reversible entropy change resulting from electrochemical reactions within the cell. The equation for the reversible heat can be written as Equation 9.

Equation 9 Reversible heat.

$$\dot{Q}_{rev} = I_{cell} T_{cell} \frac{\partial V_{OCV}}{\partial T}$$

The entropic coefficients term ($\frac{\partial V_{OCV}}{\partial T}$) is calculated from the OCV for the cell under different temperatures. The term was calculated for both charge/discharges, and the average value was used. The entropic coefficients term as a function of SOC is illustrated in Figure 14. The outlier at the beginning and end was removed, and data for SOC between 90 and 12 % was obtained in this work.

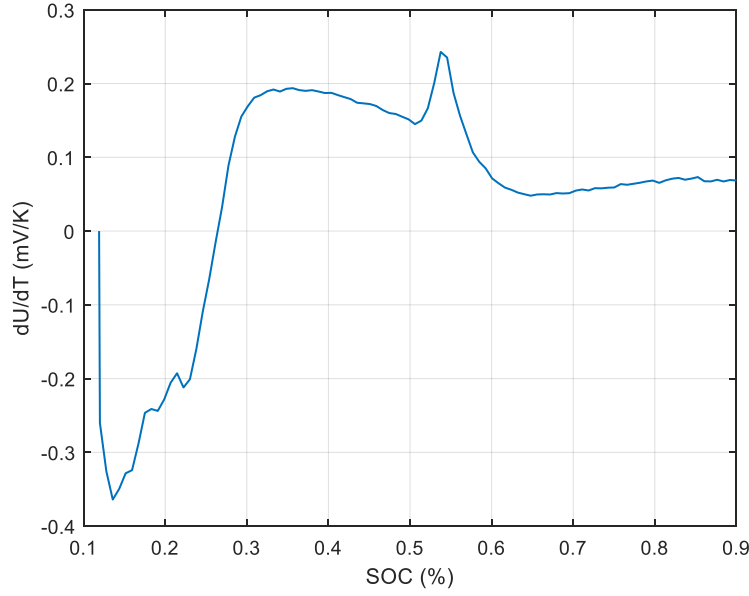


Figure 14 Entropic coefficients as a function of SOC.

Most of the time, the reversible heat considered to be negligible compared with the irreversible heat, and that depends on the material and current application. The battery studied in this work shows that the amount of heat rate disputed from the irreversible and reversible heat can vary with C-rate and is presented in Figure 15. The figure presents the heat dissipation at SOC 0.5 and the temperature of the cell around 25 °C. The reversible heat can be larger than the irreversible heat at low C-rate, so it is imported to have an accurate entropic coefficient if the thermal model is simulating at a low C-rate. However, at high C-rate, the irreversible heat is more significant and dominating, and the effect of the reversible heat is small. If the cell operates at a low C-rate, the reversible heat becomes more critical and must be considered.

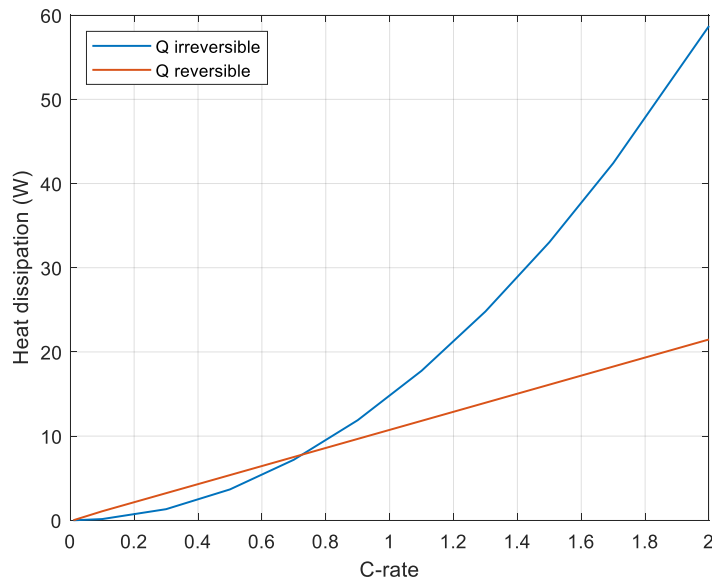


Figure 15 Heat dissipation between the irreversible and reversible as a function of C-rate.

The total heat rate from the irreversible and reversible heat for the cell is illustrated in Figure 16 with C-rate 0.5 and the temperature of the cell around 25 °C. From the figure, a noticeable result is that the reaction heats can be positive or negative within the cell due to the transfer of ions and electrons. The positive heat in the reaction is called exothermic, this occurs when there is an increase in enthalpy, and the reaction is hotter than the surrounding. The opposite happens in the endothermic reaction, where the enthalpy decreases, and the reaction is cooler than the surrounding (Santhanagopalan, Smith, Neubauer, Gi-heon, & Pescaran, 2015).

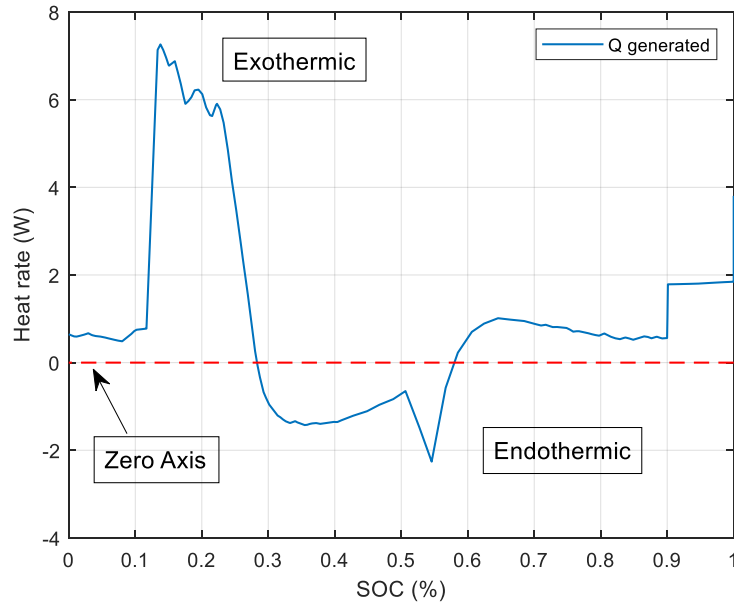


Figure 16 Cell heat rate as a function of SOC with operation C-rate at 0.5 and temperature around 25 °C.

4.2.2 Heat transfer model in the Cell

The temperature distribution in the cell depends on the material inside the cell and local heat generation. The lumped capacitance thermal model was used in the study. The cell component is illustrated in the schematic figure in Figure 17. The cell consists of five components; the jelly roll is the inside part of the cell and consists of layers of anode, cathode, and separator. The visible outside parts of the cell are the cell top, floor, and can. The visible component is integrated with the environment surrounding the cell.

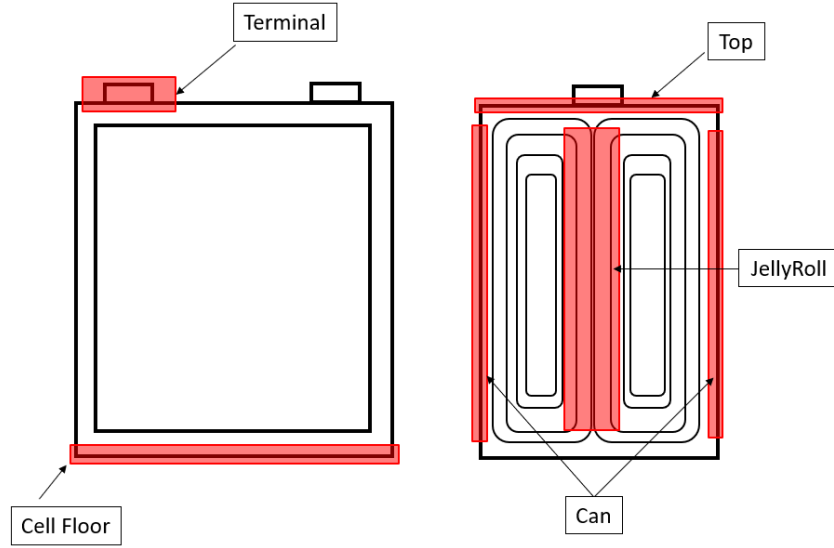


Figure 17 Schematic figure of the cell component, cell front (left), and cell side (right).

Heat transfer and the surrounding assumed to be through conductivity heat transfer (Equation 10) and convective heat transfer (Equation 11). The heat from radiation is small and assumed to be negligible. The energy balance combining the conductivity, connectivity, and heat is presented in Equation 12 (Incropera, Dewitt, Bergman, & Lavine, 2013, ss. 112-118). The definition of the symbols in the equation is presented in Table 12.

Equation 10 Conductivity heat transfer.

$$Q_{cond} = \frac{kA}{L}(T_i - T_{surf})$$

Equation 11 Convective heat transfer.

$$Q_{conv} = hA(T_{surf} - T_{amb})$$

Equation 12 Heat transfer energy balance.

$$C_{th} \frac{\partial T_i}{\partial t} = Q_{heat} - \frac{kA}{d}(T_i - T_{surf}) - hA(T_{surf} - T_{surf})$$

Table 12 Symbols description of heat transfer equations.

Symbol	Description
A	Cross-section area
C_{th}	Thermal mass capacity
h	Heat transfer coefficient
k	Thermal conductivity
L	Thickness
Q_{heat}	Thermal heat
t	Timestep
T_i	Internal temperature
T_{surf}	Surface temperature
T_{surr}	Surrounding/Ambient temperature

The cell was modeled by the thermal network shown in Figure 18, where there is one central node for the cell core (Jelly Roll), one node per face, and one for the terminal. The main heat generation happens in the cell core and transfers to the other parts of the cell, according to the figure.

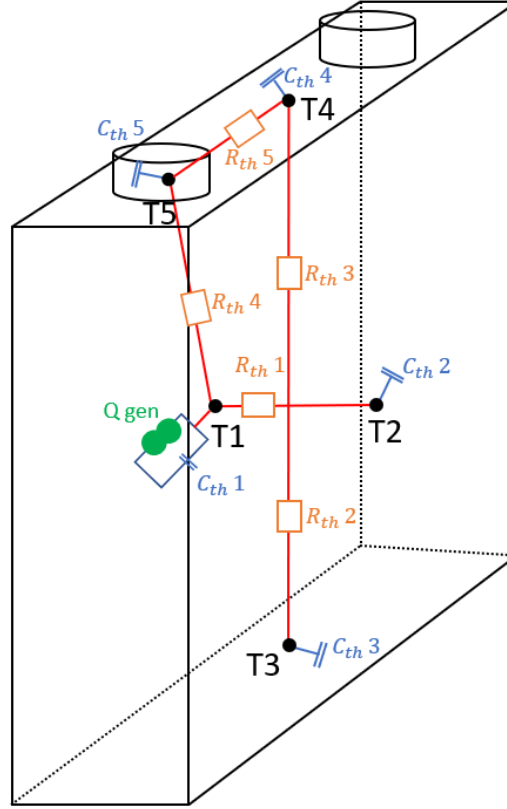


Figure 18 Lumped thermal model of the cell.

Table 13 presents the descriptions of the symbols used in Figure 18. The equation to estimate the parameter is highlighted. However, the parameter, such as thermal mass capacity (C_{th}) and thermal resistance (R_{th}) is was extracted from the cell datasheet.

Table 13 Symbols description of the lumped thermal model of the cell.

Symbol	Description	Evaluation
C_{th1}	Thermal mass capacity Jelly roll	Analytical
C_{th2}	Thermal mass capacity Can	Analytical
C_{th3}	Thermal mass capacity Cell Floor	Analytical
C_{th4}	Thermal mass capacity Top	Analytical
C_{th5}	Thermal mass capacity Terminal	Analytical
Q_{gen}	Heat generation	Estimated (Equation 7)
R_{th1}	Thermal resistance Jelly Roll – Can	Analytical
R_{th2}	Thermal resistance Can – Cell Floor	Analytical
R_{th3}	Thermal resistance Can – Top	Analytical
R_{th4}	Thermal resistance Jelly Roll – Terminal	Analytical
R_{th5}	Thermal resistance Terminal - Top	Analytical
$T1$	Temperature Jelly Roll	Estimated (Equation 12)
$T2$	Temperature Can	Estimated (Equation 12)
$T3$	Temperature Cell Floor	Estimated (Equation 12)
$T4$	Temperature Top	Estimated (Equation 12)
$T5$	Temperature Terminal	Estimated (Equation 12)

Figure 19 describes how the ECM from the battery model is used with the thermal model. The ECM is a function of SOC, current a temperature. The figure describes how the cell core, the

jelly roll is dependent on the surrounding temperature from other parts of the cell, and the heat generation from ECM. The model is dynamic and initial conditions are required.

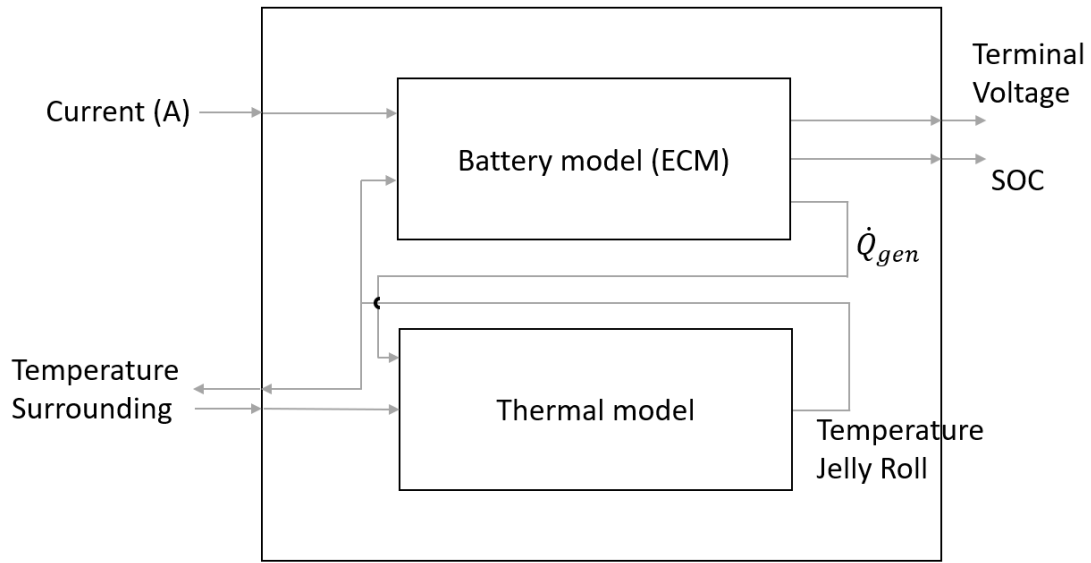


Figure 19 Coupling between the ECM, thermal model, and surrounding.

The thermal lumped model of the cell consists of heat capacity and thermal capacitance. The model describes how the heat is distributed in the cell, and therefore, the cell was not considered as a one homogeneous body. The heat generation is assumed only happened at the jelly roll, and the heat is distributed in the cell and the surroundings according to the model. Furthermore, the model is transient heat transfer, and the temperature within an object itself keeps changing with time. However, the lumped model parameters count as internal confidential information for Vattenfall and will not be illustrated in this work. The battery thermal model was developed in Simulink.

4.2.3 Cell Thermal Model Validation

The lumped model for the cell was validated using experimental data. In the experiment, the cell is kept in a chamber with a constant temperature and heat flow. A module with 12 cells was used in the test but with one cell only in operation. The module materials and surroundings were considered in the model to get as accurate as the experiment set up. The input in Simulink was the initial temperature, ambient temperature, and current for the experiment under a period of approximately 2.5 hours with 0.5 C-rate. The methodology for the validation of the cell model is presented in Figure 20.

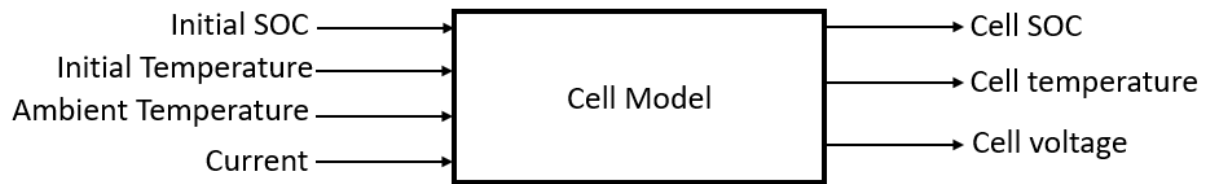


Figure 20 Methodology for cell thermal model validation.

The validation was examined by the root-mean-square deviation (RMSE). The RMSE is used to measure the differences between the operation data and simulated data. That will give how much the error is for the simulated data in the model. The average RMSE for the model is 0.38 °C. This is a relatively small difference between the experiment and simulated and is in an acceptable range. Figure 21 illustrated the temperature curve for the experiment and simulated data and RMSE with time.

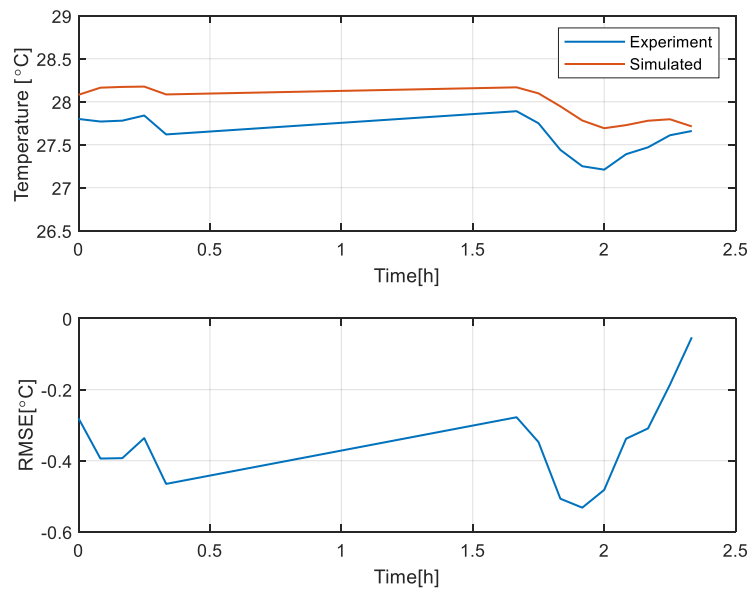


Figure 21 Cell model validation methodology.

4.3 BTMS

After when the thermal model was validated for the cell, it is applied to a battery pack. Thereby, the thermal management system was added to the thermal model for the pack. The pack used in this study is from the car company BMW used in their EV. Figure 22 shows how the battery pack looks and which components it consists of.

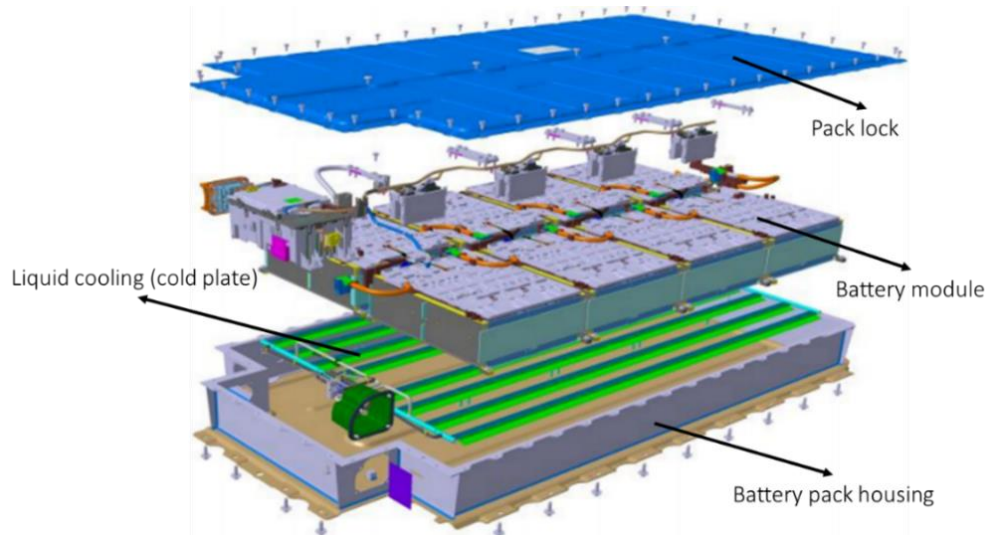


Figure 22 Battery pack used for the BTMS study (Dipl.-Ing. Florian Schoewel, 2013).

According to Figure 22, the main components used in the simulations of the battery model and BTMS are the pack lock, battery modules, cold plate, and battery pack housing. Table 14 present the general technical specifications of the studied battery pack.

Table 14 General technical specifications of the pack.

Nominal Pack capacity	120 Ah
Nominal Pack voltage	352 V
Energy content (gross/net)	42.2/37.9 kWh
Number of modules	8
Battery cell per module	12
Cooling system	Refrigerant (R134a)

The modules in the pack are surrounded by an aluminum frame, which consists of two parts, pack lock, and pack housing. Each module in the pack has an external lock called a plastic cover. These mentioned components above were vital to being considered to measure the accuracy of heat convection to the cell from ambient. Each module consists of thin aluminum module-floor. The pack has an active liquid cooling system. The cooling system uses a cold plate with a small pipe with a refrigerant coolant.

Table 15 shows the inputs data for the battery thermal model, considering the pack components material and specifications.

Table 15 Pack material and specifications

Material	plastic cover	Aluminum frame
Thickness m	0.002	0.004
Area m ²	0.1404	2.913
Density (kg/m ³)	920	-
Specific heat (J/kg, K)	1900	890
Mass (kg)	0.25834	37
Conduction coefficient (K)	0.2	218

Table 16 shows the inputs data for the battery cooling system specifications. The controller time constant means the time needed for the refrigerant to start flows into the cold plate pipes after the cell reaches a specific temperature limit.

Table 16 Battery cooling system specifications

Cooling system	Refrigerant (R134a)
One cooling pipe length	1.334 m
Cooling pipe diameter	0.026 m
cooling Pressure	5 bars
Mass flow	0.00208 kg/s
Controller time constant	17 sec
Cooling power	299.31 kW

The battery module from inside and all components around the cell looks more clearly in Figure 23. There are eight modules in the battery pack, and according to Figure 23, each battery module consists of 12 cells. The cells connected in series using busbars, and on each cell floor, there is a cold plate with two refrigerant channels, inlet, and outlet. The refrigerant at the inlet flows under all the four modules before returning as an outlet.

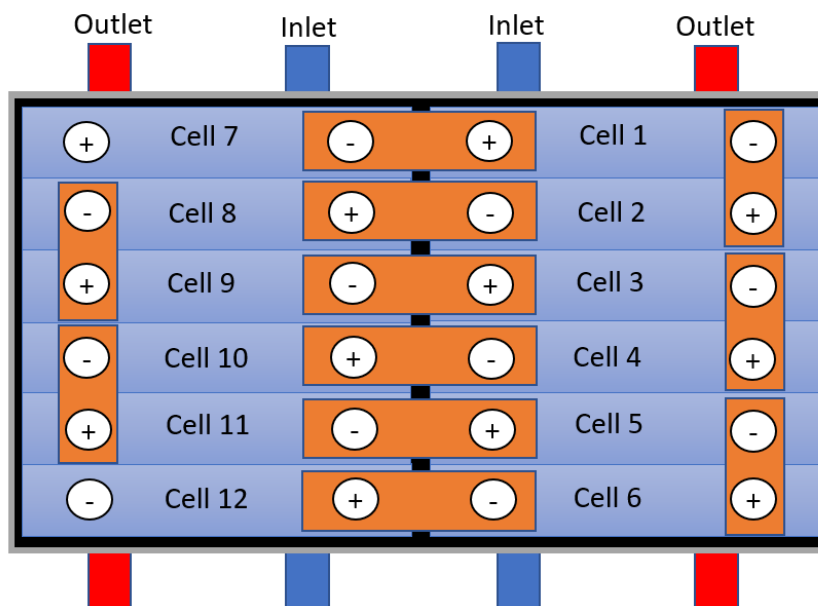


Figure 23 Battery module setup.

The Pack is a component in a refrigerant cycle. The four main components in the cycle include an evaporator, compressor, condenser, and expansion valve. The pack is the evaporator in this cycle, which works the opposite of the condenser, here refrigerant liquid is transformed to gas, absorbing heat from the modules in the pack. However, in this work, only inlet inputs such as temperature, pressure, and mass flow were taken into the model. Other another component of the refrigerant cycle was not included. This is due to limited information on the cycle and the time of the project.

4.3.1 Pack Model Validation

The air and liquid-cooling model was validated against the operational data of the battery storage container. The container house has a number of same battery pack described in the work, inverters, heat ventilation air conditioner (HVAC) system, and several other components. The HAVC system is installed to keep the container in optimal condition during cold or hot weather as well as provide cooling during peak operational time, in which both the battery pack and inverters tend to get hot. The data extracted from the system is both when the pack used air for cooling and liquid. The step size is 15 min, however smaller step size can be better for validation but was not available. The temperature data are round up and is another source of error for the validation. It is assumed there is natural convection between the room temperature and the pack aluminium frame.

The methodology for the validation of the BMW pack model is illustrated in Figure 24. The input for the simulation is the container room temperature, current, initial SOC, and initial temperature. The parameters SOC, voltage, and temperature of the top part of the cell were simulated and validated with the operation data. The top temperature part of the cell is used due to only that part of the cell had a sensor and measured temperature. The validation was examined by RMSE and determination coefficient (R^2). R^2 is used to test how good the model to predict the operation data.

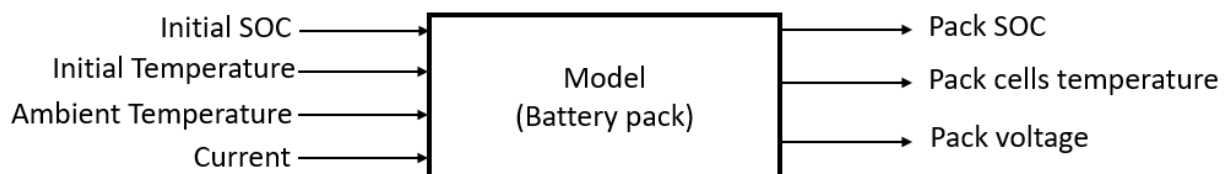


Figure 24 BMTS Pack model validation methodology.

4.3.1.1 Air Cooling Validation

Air cooling was validated against the operation data, and the result is illustrated in Table 17. The result shows that the model for air cooling is accurate and can be used for the simulation. The SOC and voltage curves are almost the same. The temperature for discharge is accurate and has RMSE mean around 0.98 °C and the charge is 0.93 °C. The R^2 is high, and the model is accurate to simulate the air cooling for the pack. The temperature curve with time for operation data and simulation for discharge is illustrated in Figure 25.

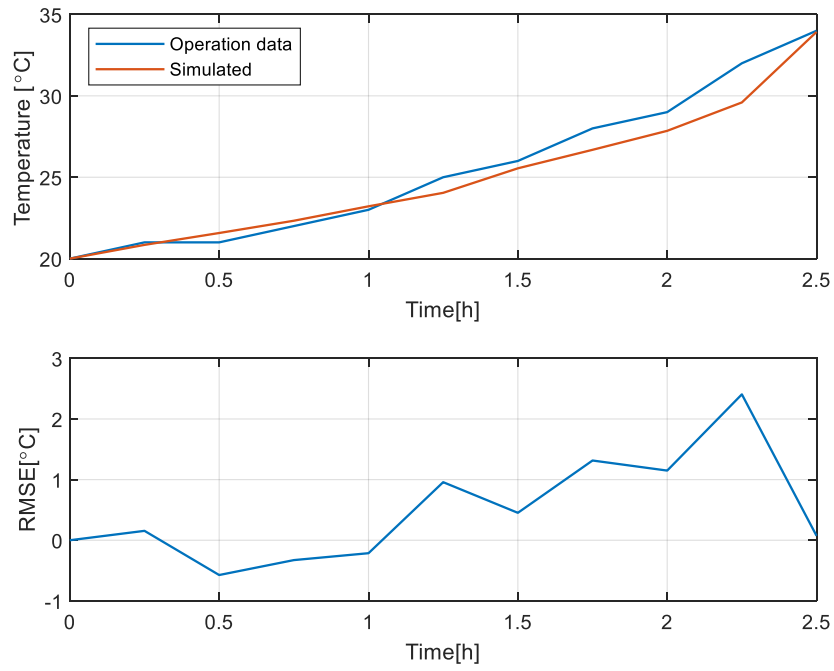


Figure 25 Air cooling temperature validation discharge

The temperature curve with time between the operation data and simulation for the charge is illustrated in Figure 26.

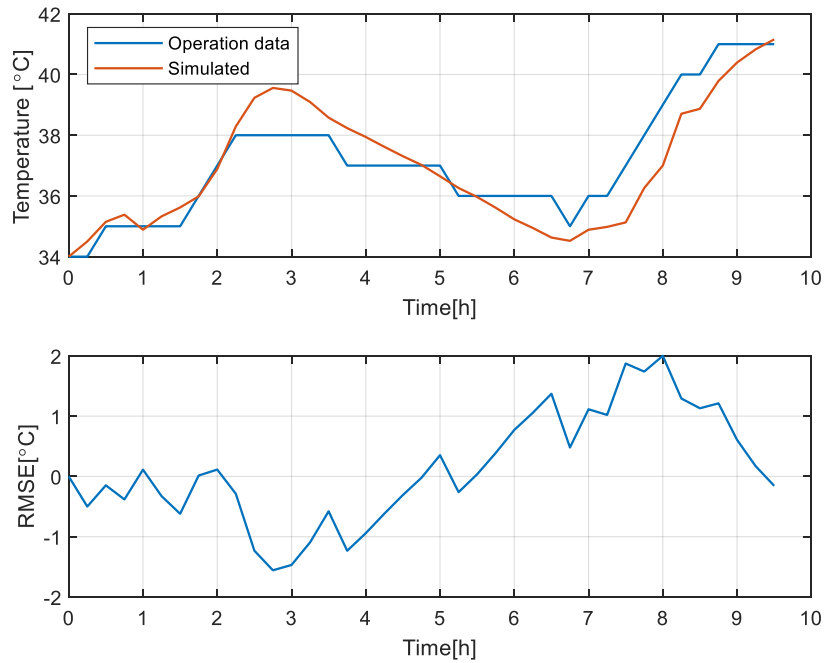


Figure 26 Air cooling temperature validation charge.

The summary of the validation for charge and discharge can be found in Table 17. The full result curves for voltage and SOC can be found in Appendix 2.

Table 17 Air cooling model validation.

Air cooling charge		
Parameters	R ²	RMSE mean
V	98%	2.58 V
SOC	99%	3.8%
T	79%	0.93 °C
Air cooling discharge		
Parameters	R ²	RMSE mean
V	98%	4.12 V
SOC	99%	5.7%
T	97%	0.98 °C

4.3.1.2 Liquid Cooling Validation

The liquid cooling is a more complicated system compared to the air cooling, and it is crucial to have the air-cooling model validated before proceeding with the liquid cooling. To be able to validate the model, the chosen data period should have enough time with liquid cooling is working. The period of the chosen data is over 17 hours, with liquid cooling working for around 5 hours. The data start with the cells are at SOC 97 % and is discharge to SOC 28%. After that, the cells are charged to SOC 97%. Figure 27 represents the temperature curve for that period and with the RMSE curve, and Table 18 represents the rest of the validation.

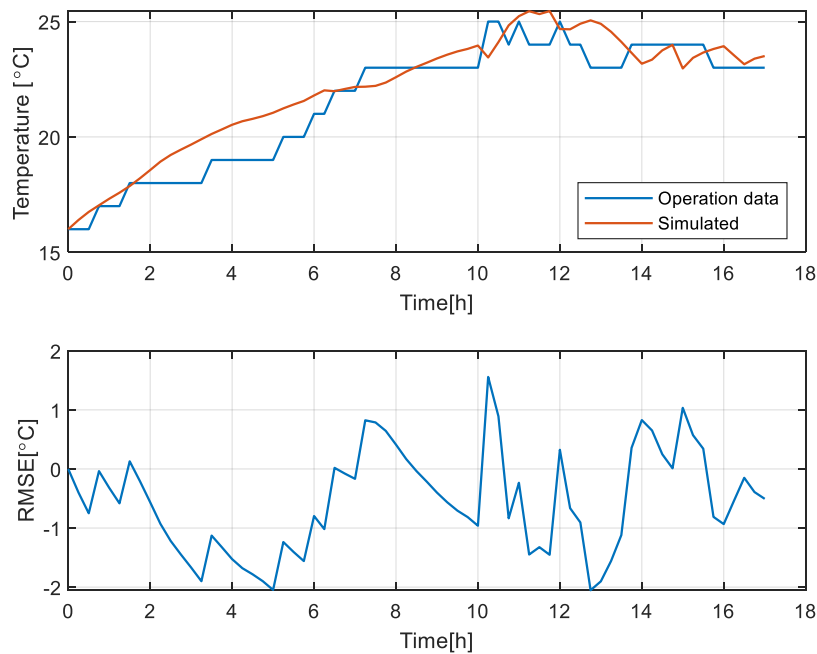


Figure 27 Liquid cooling temperature validation.

Table 18 Liquid cooling model validation.

Liquid cooling		
Parameters	R2	RMSE mean
V	98%	2.91 V
SOC	99%	2.09%
T	90%	1.02 °C

The validation curves for the SOC and voltage can be found in Appendix 2.

5 RESULTS

In this study, the terminal voltage will be simulated for the cell for the three temperature cases (0, 25, and 40 °C), and each case was simulated with different C-rate. The cell heat generation using different C-rate under different cell temperatures for both full charge and discharge cases was also studied. In addition, the cell temperature in the BMW battery pack was investigated using air, and liquid cooling simulation with the same configuration described earlier and can be seen in Figure 22.

5.1 Cell terminal voltage

The voltage curves were simulated with certain C-rate for the three cell temperatures (0, 25, and 40 °C). The result shows the impacts on the OCVs in a range of temperatures and SOC.

The result for the voltage at cell temperature 0 °C for discharge and charge is illustrated in Figure 28. From the result, the gap between OCV and terminal voltage is more significant with a higher C-rate. The gaps are resulted by the electrical resistance, which is a function of SOC and current. With a higher current, the losses are more significant.

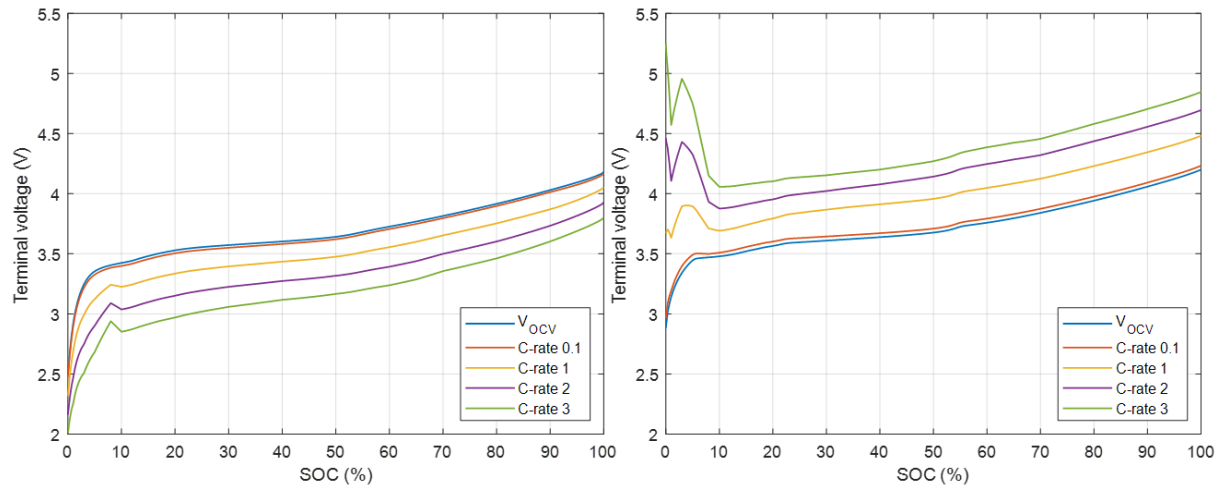


Figure 28 Voltage curve with C-rate for 0 °C, discharge (left), and charge (right).

Figure 29 presents the terminal voltage with SOC at temperature 25 °C for discharge and charge. The voltages at cell temperature 25 °C have fewer gaps compared to the 0 °C due to electrical resistance losses are smaller at higher cell temperature.

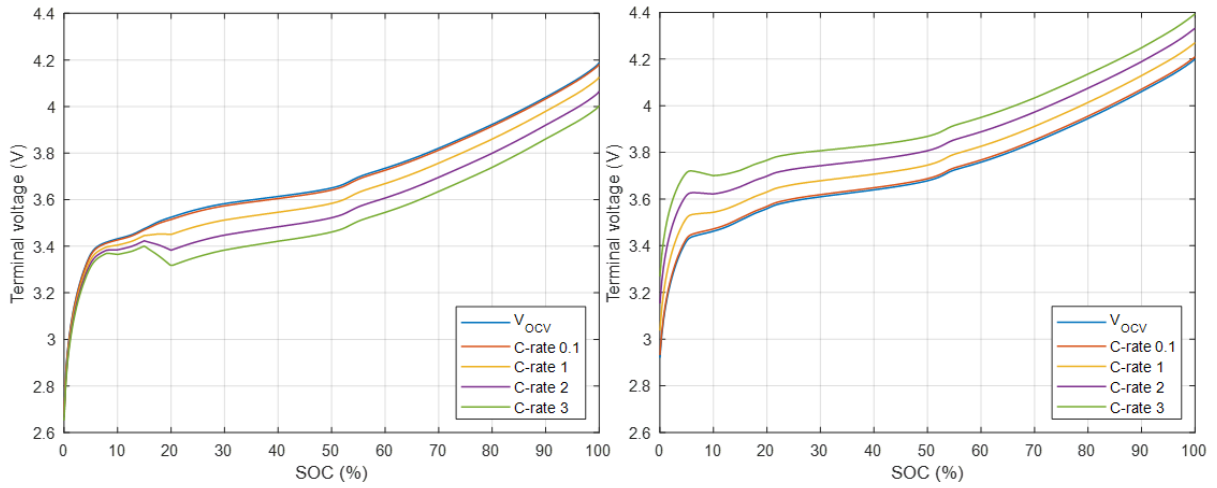


Figure 29 Voltage curve with C-rate for 25 °C, discharge (left), and charge (right).

Figure 30 shows the terminal voltage with SOC at temperature 40 °C for discharge and charge. The voltages at 40 °C have fewer gaps compared to the 0 and 25 °C due to the electrical resistance losses smaller than the other two cell temperatures.

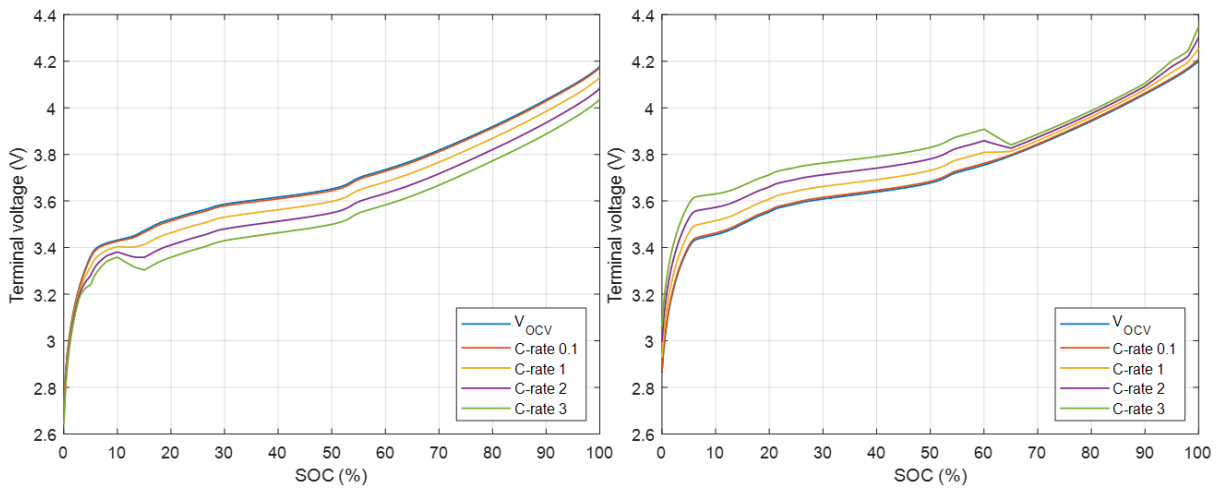


Figure 30 Voltage curve with C-rate for 40 °C, discharge (left), and charge (right).

5.2 Cell heat generation

The cell heat generation varies depending on a number of factors such as C-rate, the temperature of the cell, SOC, and if the cell is charging or discharging. In Figure 31, the cell heat generation with temperature for different C-rate is illustrated when the cell is full discharging and charging. The purpose of the figure is to see the optimum operating temperature range related to the cell generated heat. The figure shows that the cell has high heat generation at low temperature as well when the C-rate is high. However, the heat is lower at higher cell temperature, and this is due to the electrical resistances at ECM are smaller at high temperature. The optimum temperature range for the cell is between 15 and 35 °C for LIBs (Wiebelt, 2018). Another noticeable result is that heat generation from charging is higher

comparing with discharging. This is due to the electrical resistances in the ECM are higher during charge.

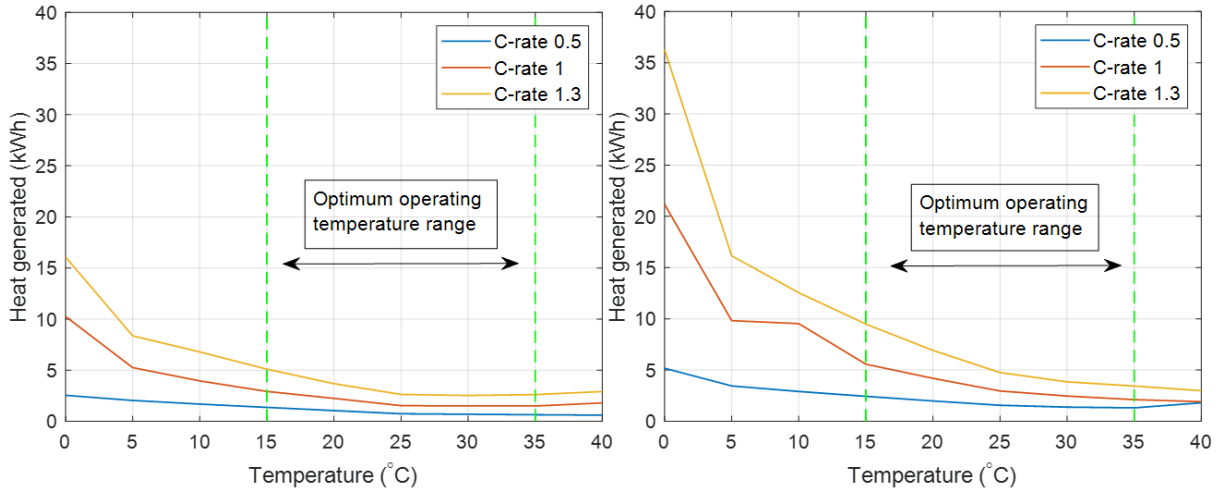


Figure 31 Cell heat generation for different C-rate with cell temperature, discharge (left) and charge (right)

5.3 Simulation result for BTMS

Simulations were conducted for the pack with different C-rate for both air and liquid cooling. The simulation result will be conducted for initial temperature, which is equal to surrounding temperatures. The temperature conditions are 12°C (T12), 18°C (T18), 22°C (T22), 28°C (T28), and 32°C (T32). The C-rate varies between 0.3 and 2. If the temperature is over 40°C, the simulation for a higher C-rate will not be recommended and can give a less accurate result. This is due to the experimental data for the ECM was conducted only for the temperatures between 0 to 40 °C.

5.3.1 Air cooling

Figure 32 illustrates the max temperature inside the cell during full discharge and charge with different C-rate. The result presented shows that the temperature of the cell depends on the surrounding temperature and the C-rate. The upper optimum temperature limit for LIBs is around 35°C and marked with a red dash line.

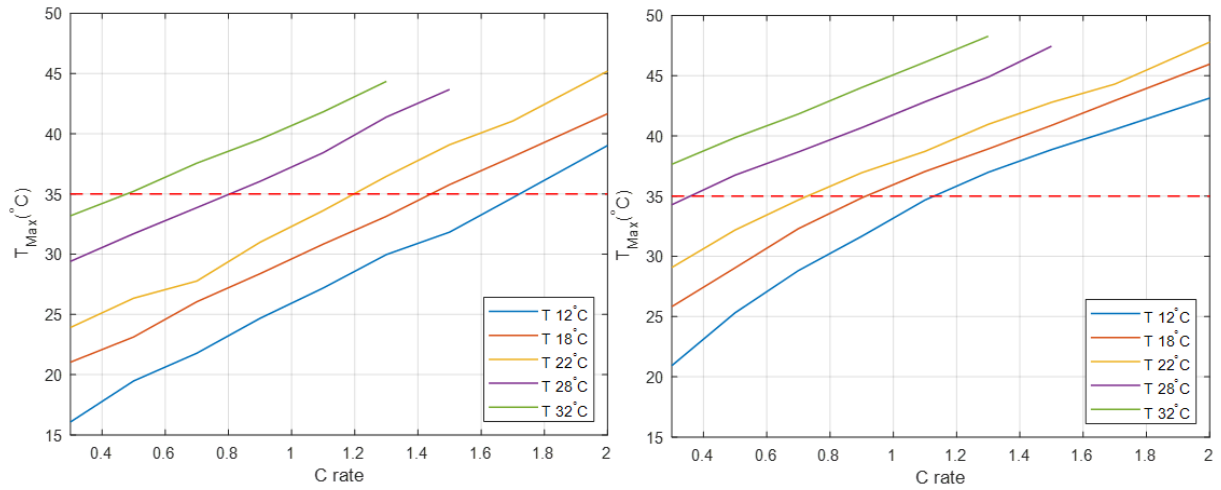


Figure 32 Max temperature of the cell using air cooling, discharge (left), and charge (right).

The maximum C-rate for every case, according to the simulation result from Figure 32, is presented in Table 19. The table shows that at lower temperature cases, the maximum C-rate is higher than in high surrounding temperature cases.

Table 19 Operation condition for air cooling.

Discharge		Charge	
Case	Max C-rate	Case	Max C-rate
T12	1.7	T12	1.15
T18	1.45	T18	0.95
T22	1.2	T22	0.75
T28	0.8	T28	0.35
T32	0.5	T32	< 0.3

Figure 33 presents the cell temperature development for different C-rate cases. The cell temperature development is the difference between max cell temperature and initial cell temperature. At low surrounding temperature cases such as at T12, the cell temperature development is higher compared to high surrounding temperature cases such as at T32 due to higher heat generation at low cell temperatures, as presented in Figure 31.

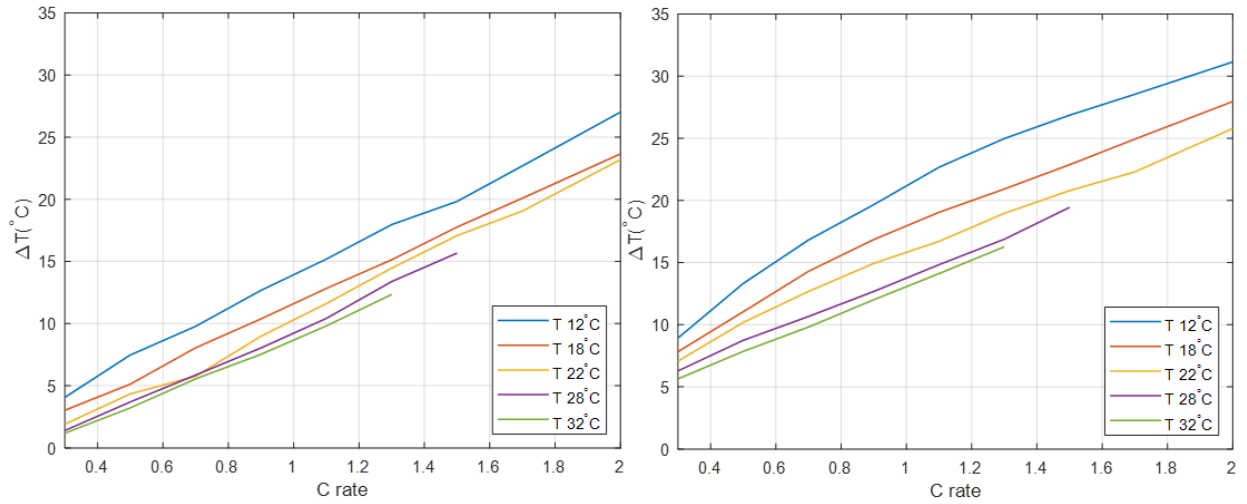


Figure 33 Temperature difference between the initial and max temperature of the cell for air cooling, discharge (left), and charge (right).

The max temperature difference within a cell is illustrated in Figure 34. The air cooling has a low-temperature difference in the cell (ΔT) and is under the upper limit of 5°C for all cases except T12 at high C-rate. However, this will not change the operation limit in Table 19.

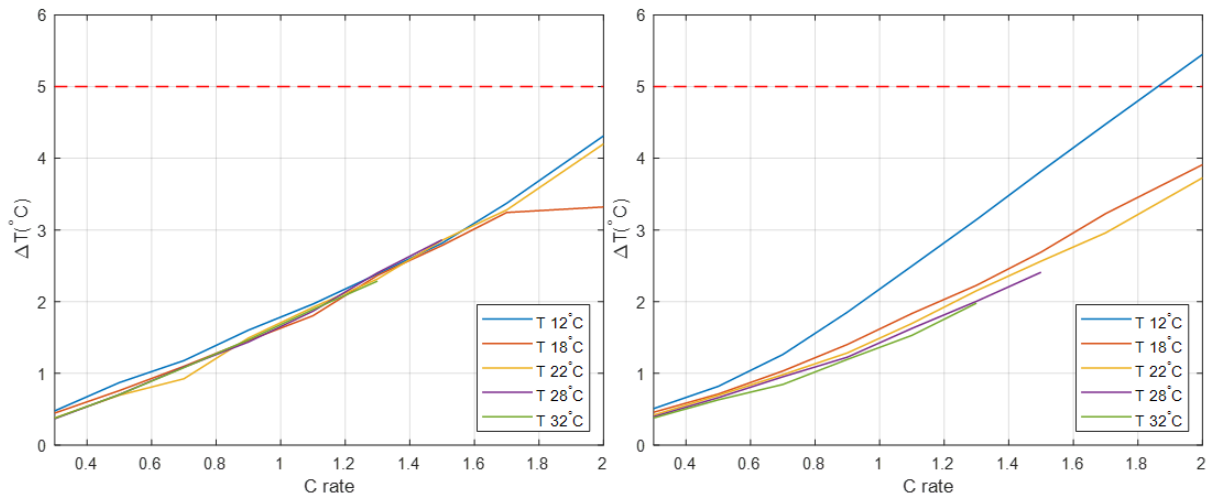


Figure 34 Max temperature difference between different parts in the of the cell for air cooling, discharge (left), and charge (right).

5.3.2 Liquid cooling

Figure 35 illustrates the cell max-temperature for surrounding temperature cases with different C-rate. The upper optimum temperature limit for LIBs is around 35°C and marked with a red dash line. The result presented shows that with liquid cooling, the cell can go for higher C-rate despite having high initial and surrounding temperature such as at T 32°C.

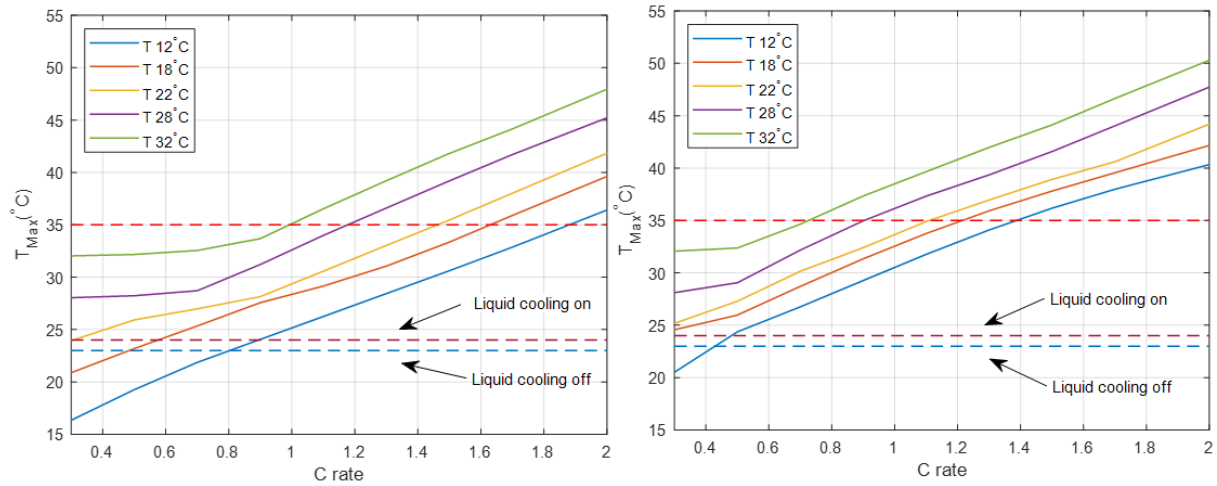


Figure 35 Max temperature of the cell using liquid cooling, discharge (left), and charge (right).

The maximum C-rate for every case, according to the simulation result from Figure 35, is presented in Table 19. The table shows that at lower surrounding temperature cases, the maximum C-rate is higher than in high surrounding temperature cases.

Table 20 Operation condition for liquid cooling.

Discharge		Charge	
Case	Max C-rate	Case	Max C-rate
T12	1.9	T12	1.38
T18	1.65	T18	1.2
T22	1.45	T22	1.1
T28	1.2	T28	0.9
T32	1	T32	0.75

Figure 36 presents the temperature development in the cell temperature. With liquid cooling, temperature development is much less compared to air cooling. The result in T28 and T32 shows that at C-rate 0.5 or lower, the cooling can have enough thermal cooling power to control the cell heat generated, and the temperature development there is almost 0 °C as seen in the figure.

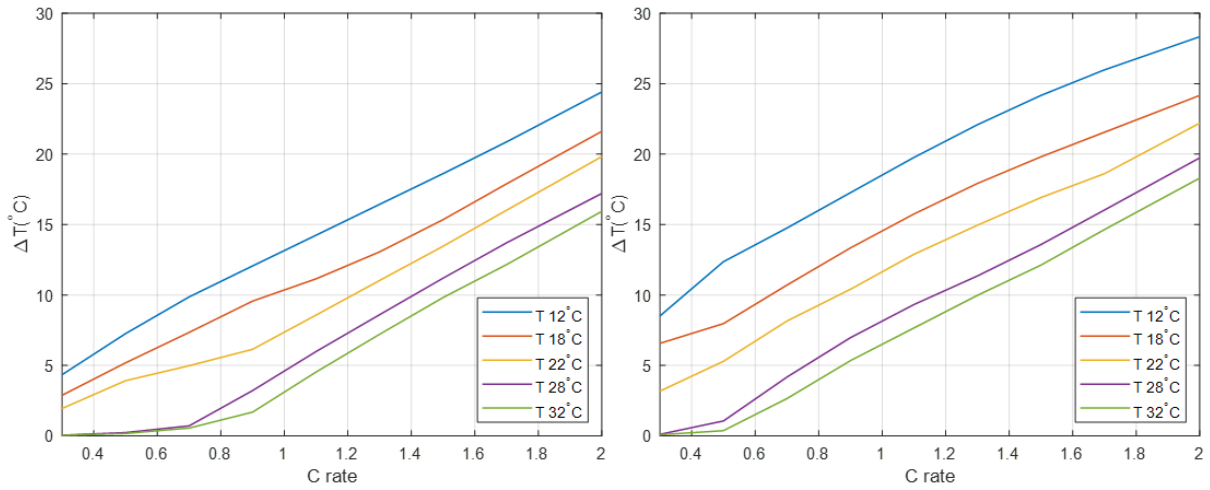


Figure 36 Temperature difference between the initial and max temperature of the cell for liquid cooling, discharge (left), and charge (right).

Figure 37 presents how the max temperature difference in the cell using liquid cooling. The result shows that liquid cooling has a high-temperature difference in the cell compared to air cooling. This is due to that the cooling plate is installed on the bottom of modules, and the prismatic cell size is big compared to other cell types. This can create a high-temperature gradient in the cell.

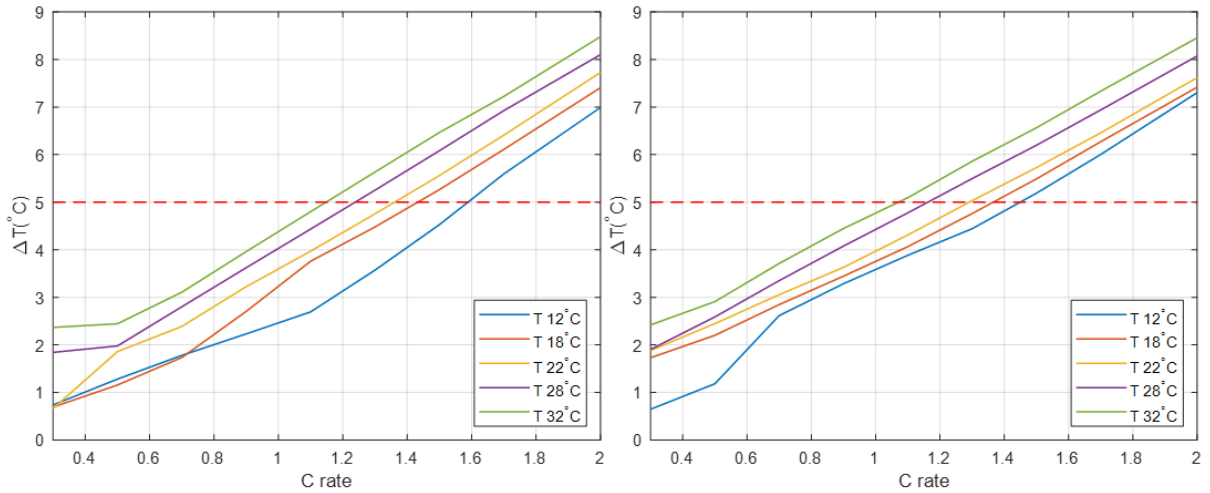


Figure 37 Max temperature difference between different parts in the of the cell for liquid cooling discharge (left), and charge (right).

According to Figure 37, there is a higher temperature difference in the cell when using liquid cooling. Thereby, the operation condition in Table 20, which only takes the 35 °C max cell optimum temperature limits to consideration, must be modified to consider the optimum maximum temperature difference in the cell of 5 degrees. The new operational condition, after taken account of both the optimum max cell temperature and maximum temperature difference in the cell, is presented in Table 21. The reduction difference after taking the temperature difference in the cell shown in the percentage in the table. The result shows that in discharge in all cases except T32, there is a reduction. For the charge cases, there is no reduction in the maximum C-rate.

Table 21 Operation condition for liquid cooling after ΔT cell.

Discharge		Charge	
Case	Max C-rate	Case	Max C-rate
T12	1.58 (-17%)	T12	1.38 (0%)
T18	1.45 (-12%)	T18	1.2 (0%)
T22	1.35 (-15%)	T22	1.1 (0%)
T28	1.25 (-7%)	T28	0.9 (0%)
T32	1 (0%)	T32	0.75 (0%)

5.3.3 Comparison between Air and Liquid cooling

A comparison between the liquid and air-cooling operating conditions was conducted from Table 21, and Table 19, with the result presented in Table 22. The result shows that air is better at T12 and T18 cases during discharge. However, in all the other cases, liquid cooling is better. The difference in optimum C-rate gets higher between liquid and air cooling with temperature surrounding get higher, this indicates air cooling is more dependent on the surrounding temperature compared using liquid cooling.

Table 22 Comparison between liquid and air cooling.

Discharge		Charge	
Case	Max C-rate	Case	Max C-rate
T12	-0.12	T12	0.28
T18	0	T18	0.3
T22	0.15	T22	0.4
T28	0.5	T28	0.55
T32	0.55	T32	>0.55

5.3.4 Relaxing period

The time for the cells to cool down in the pack with no load is expressed as a relaxing period. The simulation was conducted with the pack temperature starting at 32 °C with the surrounding temperature at 22 °C and the three cases where simulated. The first case is with the liquid cooling with natural convection outside of the pack ($h=20 \text{ W/m}^2\text{K}$). The second case is liquid turned off, and the pack is cooled by air with natural convection similar to the first condition. The last case is without liquid, and the pack is cooled by air with forced convection ($h=100 \text{ W/m}^2\text{K}$). The simulation for the cases with time is presented in Figure 38. The time for each case to cool the cells in the pack from 32 to 23 °C is presented in Table 23. The result shows that air cooling can cool the cell in a much faster time compared with only using air cooling. The result shows that there is not much between natural or forced convection with only 1.2 hours difference. This issue is due to the design of the pack being isolated with low air circulation inside and no gaps between the cells in the module for air to cool the cells.

Table 23 Cases cooling time from 32 to 23 °C

Case	Cooling time (hour)
Liquid cooling	1.8
Air cooling (natural convection)	15
Air cooling (forced convection)	13.3

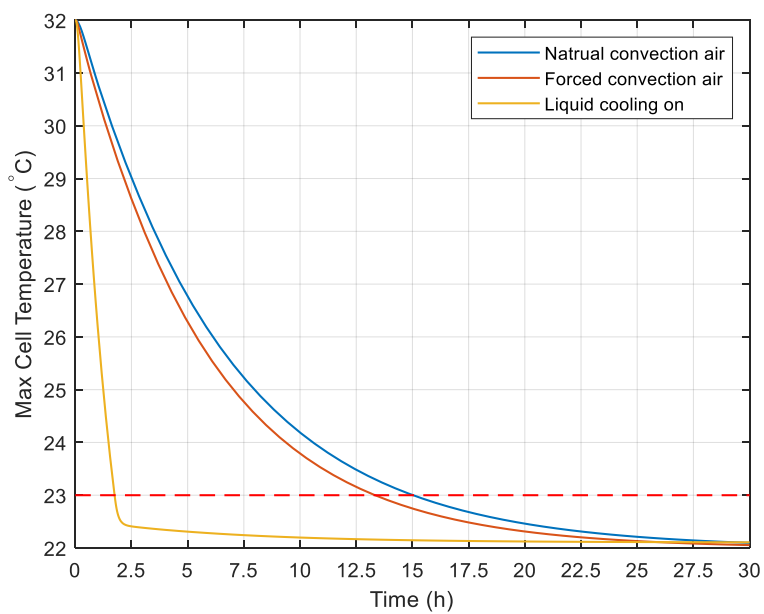


Figure 38 Relaxing period simulation

6 DISCUSSION

Most of the knowledge and industrial experiences of BTMS for LIBs come from EV applications in comparison with stationary BTMS applications. There are some differences between the EV and the grid/microgrid stationary applications, mainly in requirements, such as the scale of capacity, operation voltage, and current and battery usage patterns. Therefore, the design basis and operation requirements are different, which should further be investigated.

Actively force air cooling has mostly been used for current stationary grid/microgrid connected stationary BESS applications but with limited technical information available. The gaps in basic engineering knowledge and operation experiences could be filled by internal case studies for the existing projects and close collaboration with technology suppliers. The BMW air cooling system used in Vattenfall projects could be considered as a simple air-cooling (passive cooling) solution for the stationary application in comparison with common air-cooling concepts applied for LIB TMS.

Liquid cooling has widely been used in EV applications with different system configurations and cooling patterns. The BMW liquid cooling currently used in Vattenfall projects is a relative sample indirect liquid cooling solution in comparison with the liquid cooling systems in other EV applications. There is a general trend to increasing liquid cooling in stationary LIB TMS based on communications with some stationary BESS suppliers and users. The benefits may mainly be expected to reduce the footprint of BTMS and improve the lifetime and safety of LIBs. However, the benefits of stationary applications are not varied clear and under investigation.

It is difficult to give an apparent comparison between air cooling and liquid cooling for stationary applications without a fair comparison basis and specifying the applications because it is generally projected (service or application) dependence. The selection of a better BTMS is generally an optimization of important performance based on relevant KPIs, in which trade-offs should be made among many factors such as costs, complexity, cooling effects, temperature uniformity, and parasitic power consumption. Thermal modeling and simulation may be the best way to give a better comparison for different technical options if proper KPIs have been chosen together with economic factors.

According to the simulations, the BTMS depends on many factors such as cooling system type, the surrounding temperature, operation conditions, and C-rate. The advantages of using air cooling are that the system is a simple structure, low cost, easy maintenance, and the parasitic energy consumption is low during the system operation process due to the lower air viscosity. Moreover, according to the result, the air cooling keeps the cell temperature difference under the limit of 5°C event at high C-rate and surrounding temperature. However, the air cooling can keep the cell working under the optimum temperature only at low C-rate and low surrounding temperature. Furthermore, having low surrounding temperature can affect the heat generation in the cell, as shown in Figure 31, and can be further illustrated in Figure 33 with the temperature developed for the cell at different surrounding temperatures. The result of the air-cooling operation condition is presented in Table 19. Furthermore, it is also more

challenging to have an evenly distributed cooling performance between the cells in the pack as air has a low viscosity that makes it flow less controllable.

Using liquid cooling for the BTMS allows the cell to operate at a higher C-rate compared to air cooling since the refrigerant R134a has higher heat capacity than air. According to Figure 35, the cell can be operated at a higher C-rate and surrounding temperature, keeping the maximum temperature under the optimum limit of 35°C. Besides, according to the literature study, the liquid cooling has other advantages over air cooling such as high heat transfer, handles large cooling loads in scenarios (high power draws, high environment temperatures), better thermal balance and uniformity temperature distribution at certain conditions. The liquid cooling system also has the advantage of occupying less space compared to the air-cooling system, but it is not so crucial for BESS, where space is not limited as for EV applications. However, BTMS using liquid cooling is more complex, requires more maintenance, has a higher cost compared to air cooling, and has potential leakage, which is a safety hazard. In addition, the maximum temperature difference in the cell is higher when using liquid cooling for the BMW pack design compared to air cooling, and this is illustrated in Figure 37. The figure shows that the ΔT max in the cell at the optimum limit of 5°C and considered this shows that the maximum C-rate must be decreased for all cases for discharge except the T32 case compare with only taken the temperature max limit of 35°C into consideration. The result is illustrated in Table 21. This is due to the pack design, which makes one side of cells (cell floor) only conducting with the cold plate, and it is harder to distribute the heat through the whole-cell due to the large size of the prismatic cell. Even when using air cooling, (Lip, o.a., 2016) indicate that the cylindrical batteries achieve better performance from air cooling, since the investigated parametric influence on a cylindrical battery module due to the battery's distribution and size compared with prismatic batteries.

Furthermore, the performance comparison between the liquid and air cooling for different surrounding temperature cases is presented in Table 22. The comparison shows that using liquid cooling, the LIBs can be operated at higher C-rate and high surrounding temperature cases, such as at T32 compared to air cooling. However, the result shows that air-cooling is better at surrounding temperatures below 18°C during discharge. This due to that using liquid cooling during discharge at surrounding temperature 18°C or below will create high ΔT in the cell, above the optimum limit of 5°C. This can be seen in Table 21 at case T12 during discharge, where the max C-rate decreased by 17%.

LIBs, after many cycles, lose their capacity, and after a certain period, the cells reach end-of-life and need to recycle. If the cells do not follow their recommended operation temperature, it will appear many thermal issues that affect the performance of the cells badly. The cell operation temperature can affect the cell performance degradation at elevated temperatures, aging effects at low temperatures, thermal runaway under uncontrolled heat generation and abuse conditions, and temperature maldistribution, mostly due to BTMS setup. Finally, there is simply no BTMS solution that would fit all applications. It should instead be thoroughly investigated and optimized based on the requirements of what the system will be used for. There are several external factors when selecting a suitable thermal management system, such as the use case, cost, safety, manufacturability, life-expectancy, and other factors.

7 CONCLUSION

In this work, the status of BTMS technologies applied for stationary lithium-ion BESS was investigated. There is more literature about the BTMS for EV applications, and the major BTMS applied for stationary applications is air-cooling systems. In this study, a model for the BMW battery pack with BTMS using air and liquid cooling was developed, and the performance of the two cooling systems was compared.

The following conclusion was drawn from this work:

- Both air and liquid cooling can be applied for BESS applications with certain limits.
- The air-cooling is more suitable for the BMW battery pack operated at low surrounding temperatures or operating at low C-rate.
- The liquid cooling is better to use for the BMW battery pack operated at high surrounding temperature or operating at high C-rate. However, the cell temperature difference when using liquid cooling has a certain limitation on the operation conditions for most of the discharge cases.
- Considering air cooling, the BMW battery pack is compact, isolated, and there are no gaps between each cell for the air to flow through. This makes the BMW pack special case with passive air cooling and makes air cooling less efficient.
- There is simply no BTMS solution that would fit all applications and should be investigated and optimized based on the requirements of how and what the system will be used for.

8 FUTURE WORK

The work conducted in this thesis can be improved in several aspects. Aging factor needs to be implemented in the model. This can make the model capable of simulating and study cell capacity degradation under cells' lifetime. A more accurate study of the operational cell condition can be conducted. Furthermore, the CFD model has been developed for the cell. However, the model requires more parameters and needs more time for the BTMS system, and therefore it's not mentioned in this thesis. With the CFD model, the heat flow in the pack can be studied more in detail. In this work, the BMW pack was used for both air and liquid cooling. Furthermore, the pack is designed for liquid cooling and not air cooling. This means when using air cooling, it's passive air cooling. However, there is more pack design, such as from Samsung, that is designed for air-cooling and uses a fan to cool the cells. This is more effective than the BMW passive cooling, and this type of BTMS can be studied more and compared with the BMW liquid cooling.

REFERENCES

- Ahemd A, P. (2002). Battery thermal models for hybrid vehicle simulations. *Journal of Power Sources, Volume 110, Issue 2*, 377-382. doi:10.1016/S0378-7753(02)00200-8
- Arcus, C. (2016). *A Tale of 3 Battery Packs*. Retrieved from cleantechnica: <https://cleantechnica.com/2016/01/06/a-tale-of-3-battery-packs/>
- Aurilio, G., Gallo, D., Landi, C., Luiso, M., Rosano, A., Landi, M., & PacieHo, V. (2015). A Battery Equivalent-Circuit Model and an Advanced Technique for Parameter Estimation. *2015 IEEE International Instrumentation and Measurement Technology Conference (I2MTC) Proceedings*, 1705-1710. doi:10.1109/I2MTC.2015.7151537
- Battery university. (2019, april 24). *batteryuniversity*. Retrieved from BU-301a: Types of Battery Cells: https://batteryuniversity.com/learn/article/types_of_battery_cells
- Battery university. (2019, 07 10). *batteryuniversity*. Retrieved from BU-205: Types of Lithium-ion: https://batteryuniversity.com/learn/article/types_of_lithium_ion
- Battery, B. S. (n.d.). *Specification of C12 Fe-Battery*. Retrieved from shopify: https://cdn.shopify.com/s/files/1/0634/4605/files/BYD_ESS_and_DESS_Fe_battery_spec_201406.pdf
- Chen, D., Jiang, J., Kim, G.-H., Yang, C., & Pesaran, A. (2016). Comparison of different cooling methods for lithium ion battery cells. *Applied Thermal Engineering, Volume 94*, 846-854. doi:10.1016/j.applthermaleng.2015.10.015
- Chen, Z., Zhang, Z., & Amine, K. (2015). Chapter 1 - High Performance Lithium-Ion Batteries Using Fluorinated Compounds. *Advanced Fluoride-Based Materials for Energy Conversion*, 1-31. doi:10.1016/B978-0-12-800679-5.00001-4
- Damay, N., Forgez, C., Bichat, M.-P., Friedrich, G., & Ospina, A. (2013). Thermal modeling and experimental validation of a large prismatic Li-ion battery. *IECON 2013 - 39th Annual Conference of the IEEE Industrial Electronics Society*, 4694-4699. doi:10.1109/IECON.2013.6699893
- Damay, N., Forgez, C., Bichat, M.-P., Friedrich, G., & Ospina, A. (2013). Thermal Modeling and Experimental Validation of a Large Prismatic Li-ion Battery. *IECON 2013 - 39th Annual Conference of the IEEE Industrial Electronics Society*, 4694-4699. doi:10.1109/IECON.2013.6699893
- Dipl.-Ing. Florian Schoewel, D.-I. E. (2013). *THE HIGH VOLTAGE BATTERIES OF THE BMW i3 AND BMW i8*. Retrieved from wiki.aalto: https://wiki.aalto.fi/download/attachments/91692283/high_voltage_batteries_of_bmw_vehicles.pdf?version=1
- E, J., Han, D., Qiu, A., Zhu, H., Deng, Y., Chen, J., . . . Peng, Q. (2018). Orthogonal experimental design of liquid-cooling structure on the cooling effect of a liquid-cooled

- battery thermal management system. *Applied Thermal Engineering*, 508-520.
doi:10.1016/j.applthermaleng.2017.12.115
- E.Ciez, R., & J.F., W. (2017). Comparison between cylindrical and prismatic lithium-ion cell costs using a process based cost model. *Journal of Power Sources, Volume 340*, 273-281. doi:10.1016/j.jpowsour.2016.11.054
- Field, K. (2019). *Tesla Model 3 Battery Pack & Battery Cell Teardown Highlights Performance Improvements*. Retrieved from CleanTechnica logo:
<https://cleantechnica.com/2019/01/28/tesla-model-3-battery-pack-cell-teardown-highlights-performance-improvements/>
- Gao, Z., Chin, C., Woo, W., & Jia, J. (2017). Integrated Equivalent Circuit and Thermal Model for Simulation of Temperature-Dependent LiFePO₄ Battery in Actual Embedded Application. *Energies* 10(1), 85. doi:10.3390/en10010085
- Gatta, F., Geri, A., Lamedica, R., Lauria, S., Maccioni, M., Palone, F., . . . Ruvio, A. (2016). Application of a LiFePO₄ Battery Energy Storage System to Primary Frequency Control: Simulations and Experimental Results. *Energies*. 9, 887.
doi:10.3390/en9110887
- Guodong, X., Lei, C., & Guanglong, B. (2017). A review on battery thermal management in electric vehicle application. *Journal of Power Sources*. 367, 90-105.
doi:10.1016/j.jpowsour.2017.09.046
- Han, T., Khalighi, B., & Kaushik, S. (2017). Li-ion battery thermal management – Air vs. liquid cooling. *Second Thermal and Fluids Engineering Conference*, 1759-1772.
doi:10.1615/TFEC2017.fna.017297
- Hannan, Hoque, Hussain, Yusof, & Ker. (2018). State-of-the-Art and Energy Management System of Lithium-Ion Batteries in Electric Vehicle Applications. *Issues and Recommendations," in IEEE Access*, vol. 6, 19362-19378.
doi:10.1109/ACCESS.2018.2817655
- Hirota, S., Hara, K., Ochida, M., & Mishiro, Y. (2015). Energy storage system with cylindrical large formatted lithium ion batteries for industrial applications. *2015 IEEE International Telecommunications Energy Conference (INTELEC)*, 1-6.
doi:10.1109/INTLEC.2015.757236
- Huaqiang, L. Z. (2017). Thermal issues about Li-ion batteries and recent progress in battery thermal management systems: A review. *Energy Conversion and Management, Volume 150*, 304-330. doi:10.1016/j.enconman.2017.08.016
- Huria, Ceraolo, Gazzarri, & Jackey. (2012). High Fidelity Electrical Model with Thermal Dependence for Characterization and Simulation of High Power Lithium Battery Cells. *2012 IEEE International Electric Vehicle Conference*, 1-8.
doi:10.1109/IEVC.2012.6183271

- Hwang, H.-Y., Chen, Y.-S., & Chen, J.-S. (2014). Optimizing the Heat Dissipation of an Electric Vehicle Battery Pack. *Advances in Mechanical Engineering*. 7, 204131-204131. doi:10.1155/2014/204131
- Incropera, F., Dewitt, D., Bergman, T., & Lavine, A. (2013). *Principles of HEAT and MASS TRANSFER* (Vol. Seventh edition). Wiley.
- Jongerden, M., & Haverkort, B. (2009). Which battery model to use? *IET Software*, vol. 3, no. 6, 445-457. doi:10.1049/iet-sen.2009.0001
- K.Takei, K.Kumai, Y.Kobayashi, H.Miyashiro, N.Terada, T.Iwahori, & T.Tanaka. (2001). Cycle life estimation of lithium secondary battery by extrapolation method and accelerated aging test. *Journal of Power Sources Volumes 97-98*, 697-701. doi:10.1016/S0378-7753(01)00646-2
- Kai, C., Weixiong, W., Fang, Y., Lin, C., & Shuangfeng, W. (2019). Cooling efficiency improvement of air-cooled battery thermal management system through designing the flow pattern. *Energy, Volume 167*, 781-790. doi:10.1016/j.energy.2018.11.011
- Keil, P., Schuster, S. F., Wilhelm, J., Travi, J., Hauser, A., Karl, R. C., & Jossen, A. (2016). Calendar Aging of Lithium-Ion Batteries: I. Impact of the Graphite Anode on Capacity Fade. *Journal of The Electrochemical Society* 163(9), A1872-A1880. doi:10.1149/2.0411609jes
- Khan, R., Nielsen, M. P., & Kær, S. K. (2014). Feasibility Study and Techno-economic Optimization Model for Battery Thermal Management System. . *Proceedings of the 55th Conference on Simulation and Modelling (SIMS 55), Modelling, Simulation and Optimization, Aalborg, Denmark.*, Volume: Issue: 108 Article No.: 002. doi:10.13140/2.1.4909.2166
- Kim, Y., Ho, T., Marina, T., & Eugene, T. (2012). Comparative Study on Thermal Behavior of Lithium-Ion Battery Systems With Indirect Air Cooling and Indirect Liquid Cooling. *ASME/ISCIE 2012 International Symposium on Flexible Automation*, 585-591. doi:10.1115/ISFA2012-7196
- Lighting Global. (2019, June). *Lithium-ion Batteries Part I: General overview and 2019 update*. Retrieved from https://www.lightingglobal.org/wp-content/uploads/2019/06/Lithium-Ion_TechNote-2019_update-1.pdf
- Lip, H. S., Yonghuang, Y., Andrew A.O, T., Wen Tong, C., Seng How, K., & Ming Chian, Y. (2016). Computational fluid dynamic and thermal analysis of Lithium-ion battery pack with air cooling. *Applied Energy, Volume 177*, 783-792. doi:10.1016/j.apenergy.2016.05.122
- Low Wen, Y., Aziz, J., Pui Yee, K., & N. R. N., I. (2013). Modeling of Lithium-Ion Battery Using MATLAB/Simulink. *IECON 2013 - 39th Annual Conference of the IEEE Industrial Electronics Society*, 1729-1734. doi:10.1109/IECON.2013.6699393

- Maan, A.-Z., Ibrahim, D., & Marc A, R. (2018). Thermal management systems for batteries. *International Journal of Energy Research* Volume 42, Issue 10, 3143-3410. doi:10.1002/er.4095
- Madani, S. S., Swierczynski, M. J., & Kær, S. K. (2017). A review of thermal management and safety for lithium ion batteries. *Twelfth International Conference on Ecological Vehicles and Renewable Energies (EVER)*., 1-20.
- Makinejad, K., Arunachala, R., Arnold, S., Ennifar, H., Zhou, H., Jossen, A., & Wen, C. (2015). A Lumped Electro-Thermal Model for Li-Ion Cells in Electric Vehicle Application. *World Electric Vehicle Journal*. 7, 1-13. doi:10.3390/wevj7010001
- Meng, S. (2018). *KTH website*. Retrieved from <https://www.kth.se/ket/nuclear/diploma-projects/technical-survey-of-thermal-effects-and-management-of-lithium-ion-batteries-in-stationary-energy-storage-systems-1.826020>
- Miao, Y., Hynan, P., Von Jouanne, A., & Yokochi, A. (2019). Current Li-ion battery technologies in electric vehicles and opportunities for advancements. *Energies* 12(6), 1074-1094. doi:10.3390/en12061074
- Ning, G., Haran, B., & N.Popov, B. (2003). Capacity fade study of lithium-ion batteries cycled at high discharge rates. *Journal of Power Sources* Volume 117, 160-169. doi:10.1016/S0378-7753(03)00029-6
- Ouyang, D., Chen, M., Huang, Q., Weng, J., Wang, Z., & Wang, J. (2019). A Review on the Thermal Hazards of the Lithium-Ion Battery and the Corresponding Countermeasures. *Applied Sciences*, 9(12), 2483. doi:10.3390/app9122483
- Panigrahi, D., Chiasserini, C., Dey, S., Rao, R., Raghunathan, A., & Lahiri, K. (2001). Battery Life Estimation of Mobile Embedded Systems. *VLSI Design 2001. Fourteenth International Conference on VLSI Design*, 57-63. doi:10.1109/ICVD.2001.902640
- Qian, Z., Li, Y., & Rao, Z. (2016). Thermal performance of lithium-ion battery thermal management. *Energy Conversion and Management*, Volume 126, 622-631. doi:10.1016/j.enconman.2016.08.063
- qnovo. (2015). *INSIDE THE BATTERY OF A NISSAN LEAF*. Retrieved from qnovo: <https://qnovo.com/inside-the-battery-of-a-nissan-leaf/>
- R.Belt, J., D.Ho, C., G.Motloch, C., J.Miller, T., & Q.Duong, T. (2003). A capacity and power fade study of Li-ion cells during life cycle testing. *Journal of Power Sources* Volume 123, 241-246. doi:10.1016/S0378-7753(03)00537-8
- Rancilio, G., Lucas, A., Kotsakis, E., Fulli, G., Merlo, M., Delfanti, M., & Masera, M. (2019). Modeling a Large-Scale Battery Energy Storage System for Power Grid Application Analysis. *Energies*. 12, 3312. doi:3312. 10.3390/en12173312

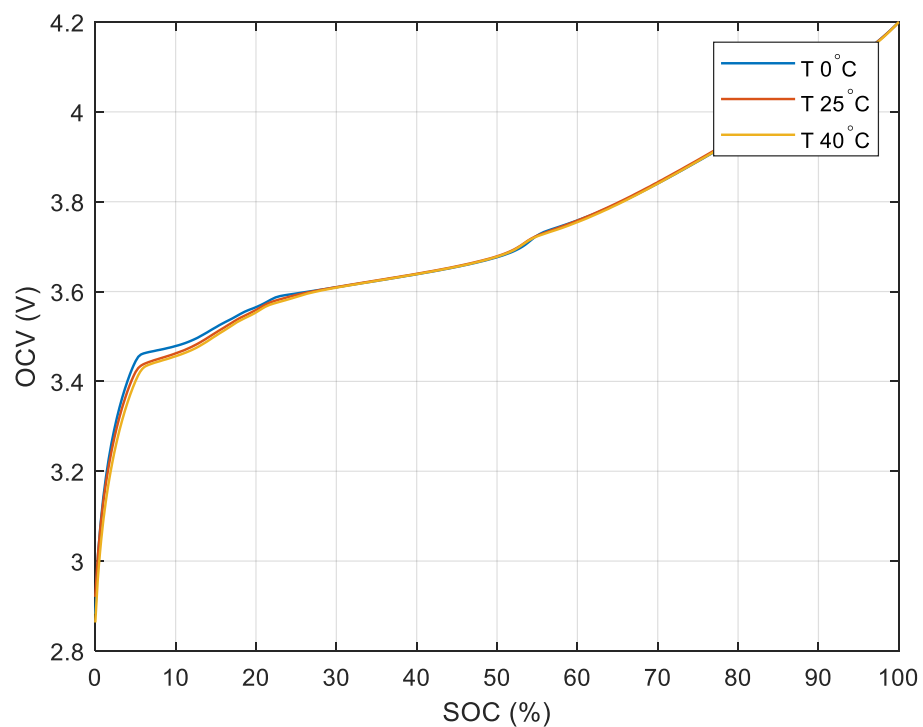
- Rao, V., Singhal, G., Kumar, A., & Navet, N. (2005). Battery Model for Embedded Systems. *18th International Conference on VLSI Design held jointly with 4th International Conference on Embedded Systems*, 105-110. doi:10.1109/ICVD.2005.61
- relionbattery. (2019). *relionbattery*. Retrieved from Lithium-Ion Cylindrical Cells Vs. Prismatic Cells: <https://relionbattery.com/blog/lithium-ion-cylindrical-cells-vs-prismatic-cells>
- S.Panchal, R.Khasow, I.Dincer, M.Agelin-Chaab, R.Fraser, & M.Fowler. (2017). Numerical modeling and experimental investigation of a prismatic battery subjected to water cooling. *An International Journal of Computation and Methodology*, 626-637. doi:10.1080/10407782.2016.1277938
- safecloudenergy. (2018). *BYD LiFePO₄ battery Module/Cell*. Retrieved from safecloudenergy: <http://www.safecloudenergy.com/index.php/product/index/g/e/id/15.html>
- Samsung. (2017). *samsungsdi*. Retrieved from samsungsdi: <https://www.samsungsdi.com/ess/index.html>
- Samsung. (2018). *samsungsdi*. Retrieved from Samsung SDI: http://www.samsungsdi.com/upload/ess_brochure/201803_SamsungSDI%20ESS_EN.pdf
- Santhanagopalan, S., Smith, K., Neubauer, J., Gi-heon, K., & Pescaran, A. (2015). *Design and Analysis of Large Lithium-ion Battery Systems (Power Engineering)*. Artech House.
- Schuster, P., Wilhelm, S., Travi, J., Hauser, J., Karl, A., & R.C. Jossen, A. (2016). Calendar aging of lithium-ion. *Journal of The Electrochemical Society*, 163 (9), A1872-A1880. doi:10.1149/2.0411609jes
- Seyed Saeed, M., Maciej Jozef, S., & Søren, K. K. (2017). A review of thermal management and safety for lithium ion batteries. *2017 Twelfth International Conference on Ecological Vehicles and Renewable Energies (EVER)*, 1-20. doi:10.1109/EVER.2017.7935914
- Team, M. E. (2008). *web.mit.edu*. Retrieved from A Guide to Understanding Battery Specifications: http://web.mit.edu/evt/summary_battery_specifications.pdf
- Tesla. (n.d.). *Powerpack*. Retrieved from Tesla: <https://www.tesla.com/powerpack>
- Tesvolt. (2018). *LITHIUM STORAGE SYSTEM TS HV 70*. Retrieved from Tesvolt: <https://www.tesvolt.com/en/>
- Todd M., B., Srinivas, G., & Thomas F., F. (2011). A Critical Review of Thermal Issues in Lithium-Ion Batteries. *Journal of The Electrochemical Society* 158(3):R1. doi:10.1149/1.3515880

- Torre, W. (2015). *Center for Energy Research University of California – San Diego*. Retrieved from Sandia: https://www.sandia.gov/ess-ssl/docs/pr_conferences/2015/PR%204/2-Torre.pdf
- University Of Washington. (2020). *Clean Energy Institute*. Retrieved from <https://www.cei.washington.edu/education/science-of-solar/battery-technology/>
- V. Reddy, M., Mauger, A., M. Julien, C., Paoletta, A., & Zaghbi, K. (2020). Brief History of Early Lithium-Battery Development. *Materials* 2020,13,1884, 1884. doi:10.3390/ma13081884
- Wang, Z., Ma, J., & Zhang, L. (2017). Finite Element Thermal Model and Simulation for a Cylindrical Li-Ion Battery. *IEEE Access*, vol. 5, 15372-15379. doi:10.1109/ACCESS.2017.2723436
- Wiebelt, A. (2018). Battery thermal management. *Lithium-Ion Batteries: Basics and Applications*, 155-164. doi:10.1007/978-3-662-53071-9_13
- VOLT, C. (2016). *CHEVROLET VOLT*. Retrieved from media: https://media.gm.com/content/dam/Media/microsites/product/Volt_2016/doc/VO LT_BATTERY.pdf
- Xianxia, Y., Hansan, L., & Jiujiu, Z. (2011). *LITHIUM-ION BATTERIES: Advanced Material and Technologies*. CRC Press, Taylor & Francis Group: New York.
- Xiaosong, H., Shengbo, L., & Huei, P. (2012). A comparative study of equivalent circuit models for Li-ion batteries. *Journal of Power Sources*, Volume 198, 359-367. doi:10.1016/j.jpowsour.2011.10.013
- Xuning, F., Mou, F., Xiangming, H., & Languang, L. (2014). Thermal runaway features of large format prismatic lithium ion battery using extended volume accelerating rate calorimetry. *Journal of Power Sources*. 255, 294–301. doi:10.1016/j.jpowsour.2014.01.005
- Yang, S., Ling, C., Fan, Y., Yang, Y., Tan, X., & Dong, H. (2019). A Review of Lithium-Ion Battery Thermal Management System Strategies and the Evaluate Criteria. *International Journal of Electrochemical Science*, 6077-6107. doi:10.20964/2019.07.06
- Yanga, D., Wang, Y., Pan, R., Chen, R., & Chen, Z. (2017). A neural network based state-of-health estimation of lithium-ion battery in electric vehicles. *Energy Procedia*, Volume 105, 2059-2064. doi:10.1016/j.egypro.2017.03.583
- You, H., Bae, J., Cho, S., Lee, J., & Kim, S.-H. (2018). Analysis of equivalent circuit models in lithium-ion batteries. *AIP Advances*. 8, 125101. doi:10.1063/1.5054384
- Zhang, Q., Shang, Y., Duan, B., & Zhang, C. (2018). An improved Peukert battery model of nonlinear capacity considering temperature effect. *IFAC PapersOnLine*, Volume 51, Issue 31,, 665-669. doi:10.1016/j.ifacol.2018.10.154

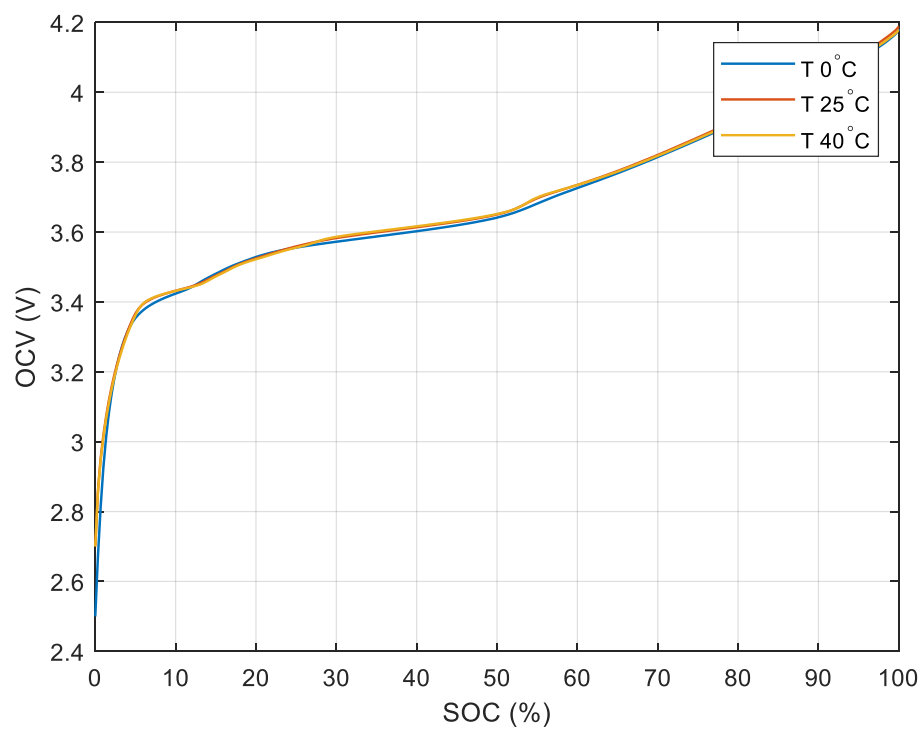
- Zhang, S., Xu, K., & Jow, T. (2003). Low-temperature performance of Li-ion cells with a LiBF₄-based electrolyte. *Journal of Solid State Electrochemistry - J SOLID STATE ELECTROCHEM.* 7, 147–151. doi:10.1007/s10008-002-0300-9
- Zhengming John, Z., Premanand, R., & Weifeng, F. (2014). Lithium-Ion Batteries. *Advances and Applications*, 409-435. doi:10.1016/B978-0-444-59513-3.00018-2
- Zhonghao, R., & Shuangfeng, W. (2011). A review of power battery thermal energy management. *Renewable and Sustainable Energy Reviews, Volume 15, Issue 19*, 4554-4571. doi:10.1016/j.rser.2011.07.096
- Zhoujian, A., Li, J., Yong, D., Chao, D., & Xuejiao, L. (2017). A Review on Lithium-ion Power Battery Thermal Management Technologies. *Journal of Thermal Science*, 391-412. doi:10.1007/s11630-017-0955-2
- Zou, C., Manzie, C., & Nesic, D. (2015). PDE battery model simplification for charging strategy evaluation. *10th Asian Control Conference (ASCC)*, 1-6. doi:10.1109/ASCC.2015.7244553

Appendix 1: OCV Measurement

OCV charge curve with SOC

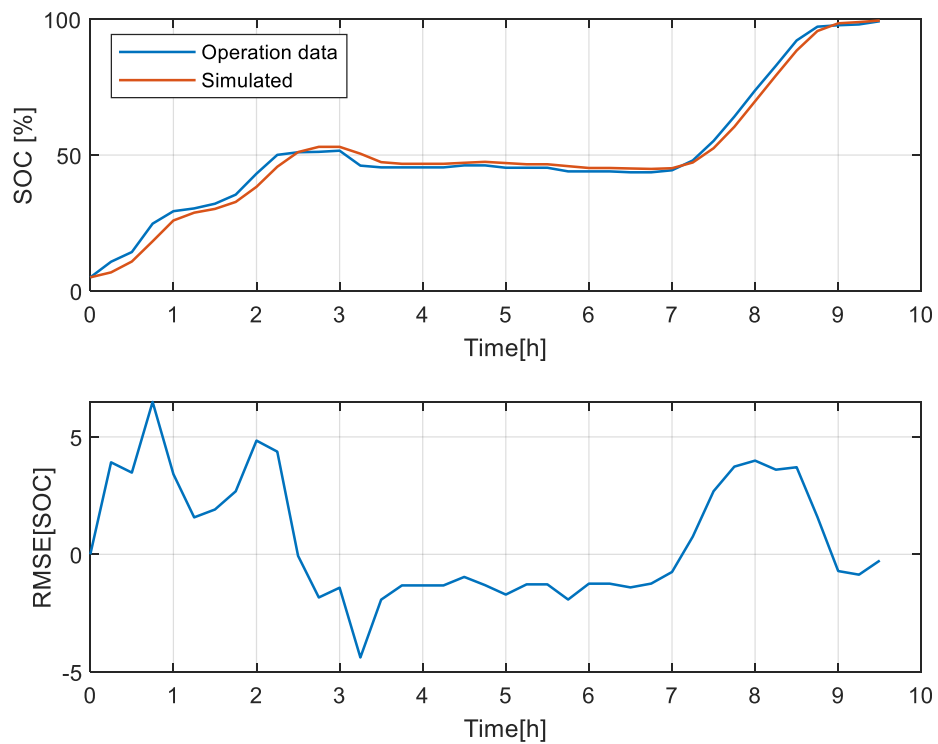


OCV charge curve with SOC

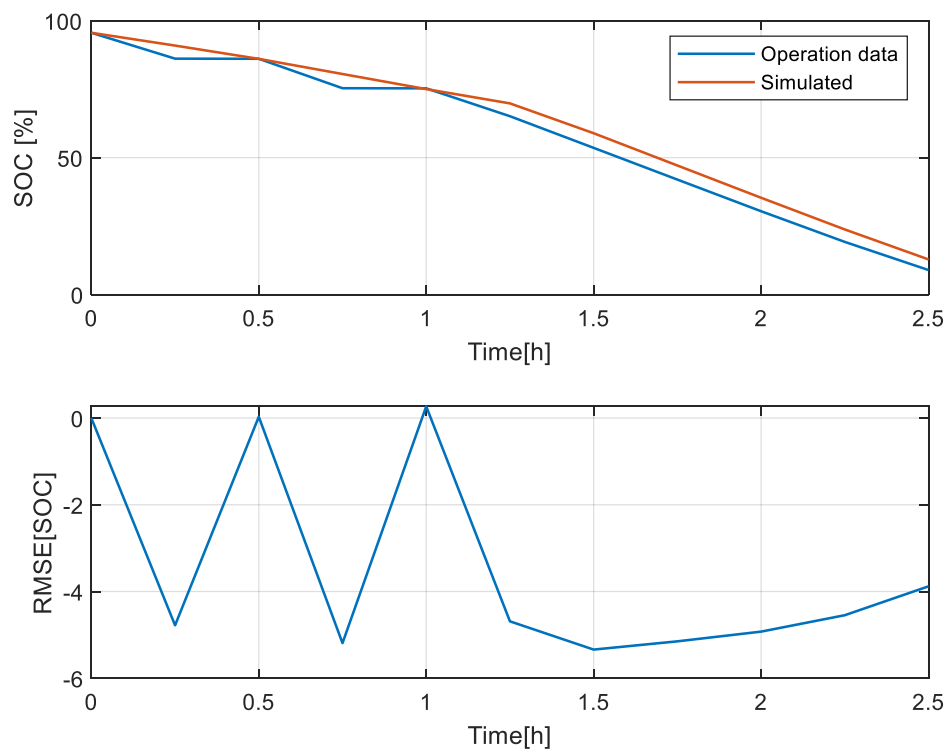


Appendix 2: Operation data validation

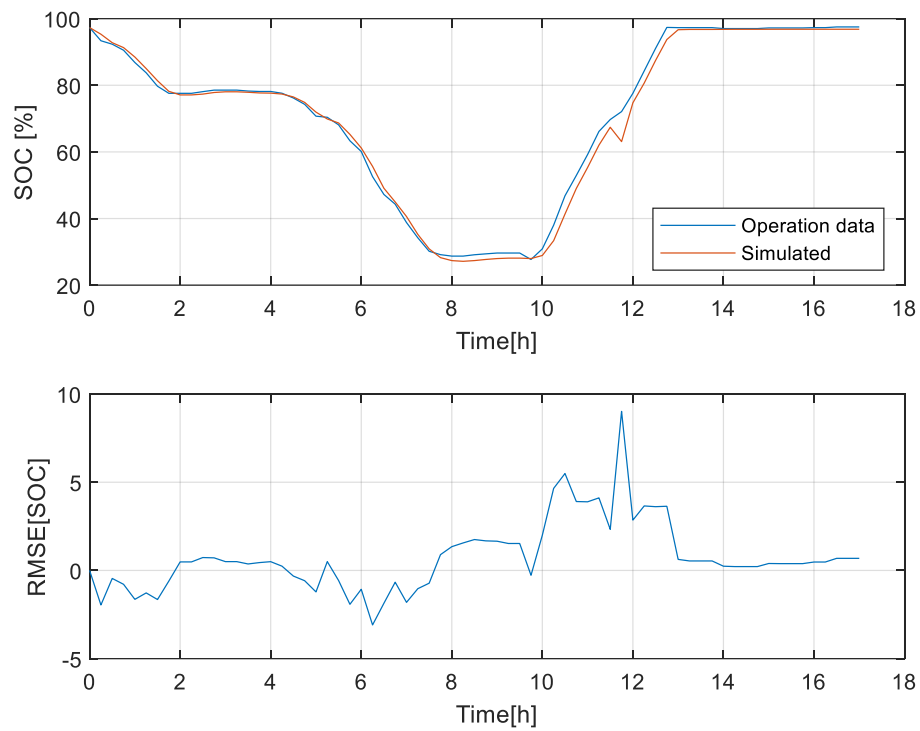
Air Cooling SOC Charge



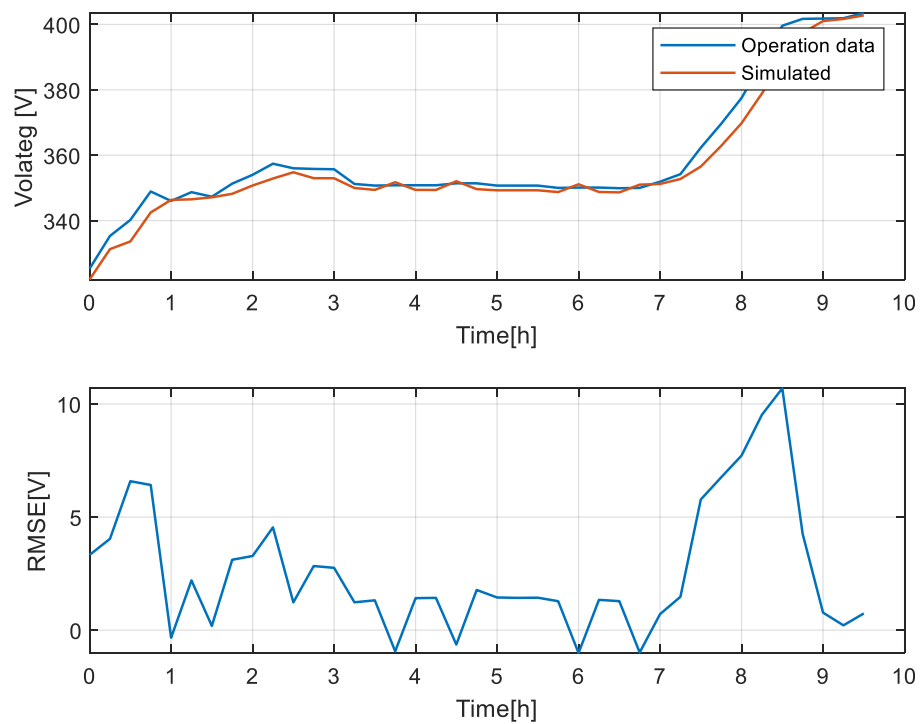
Air Cooling SOC Discharge



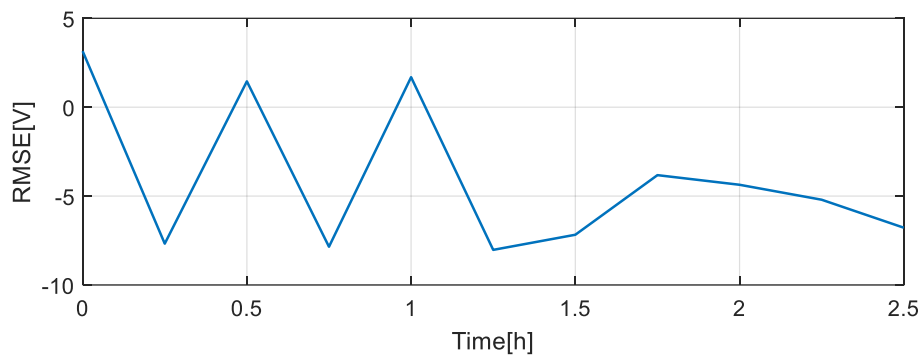
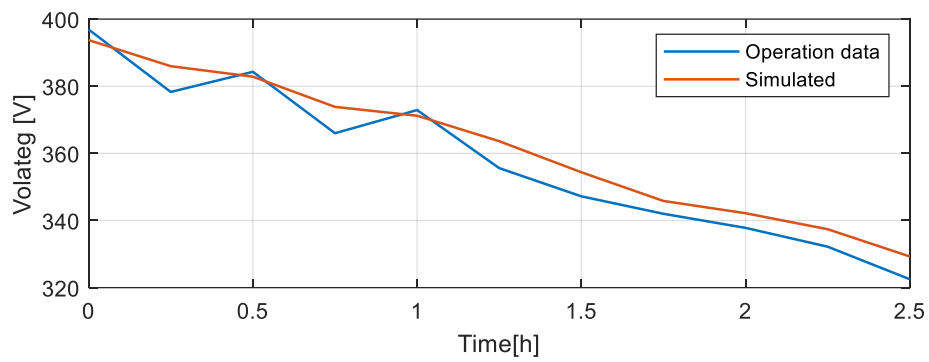
Liquid Cooling SOC



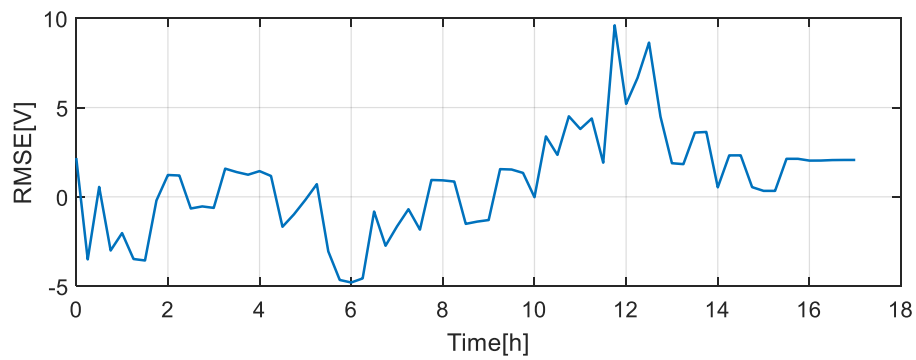
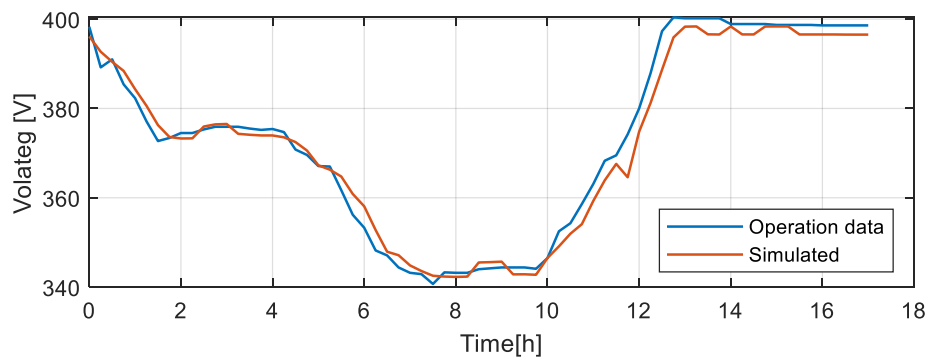
Air Cooling Voltage Charge



Air Cooling Voltage Discharge

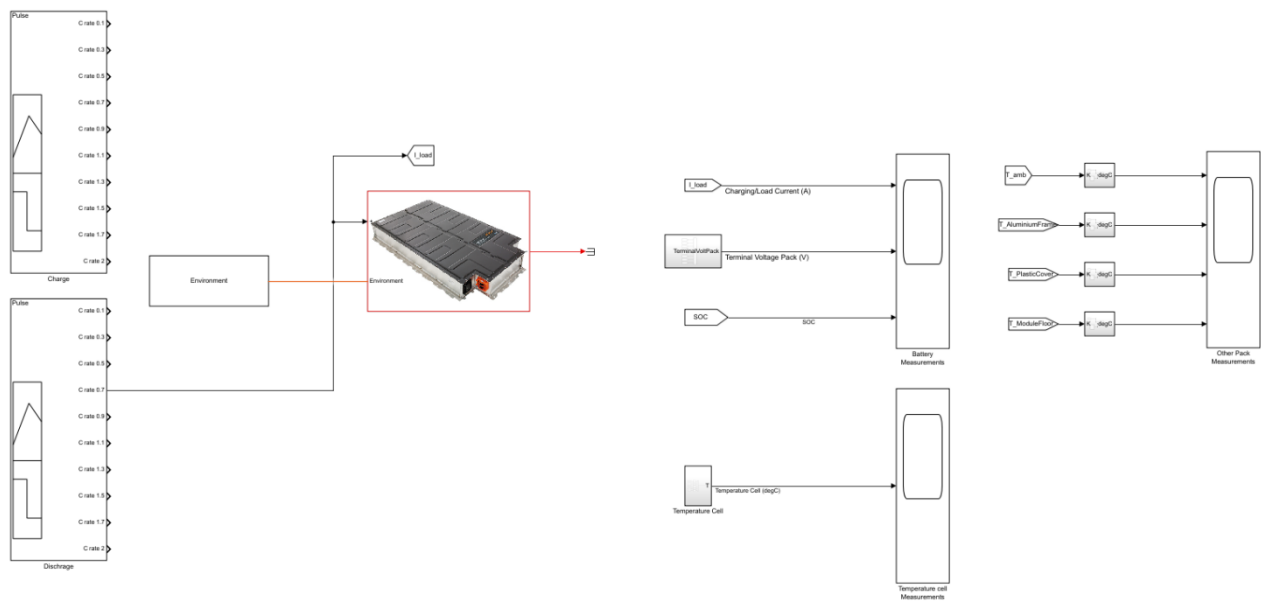


Liquid Cooling Voltage

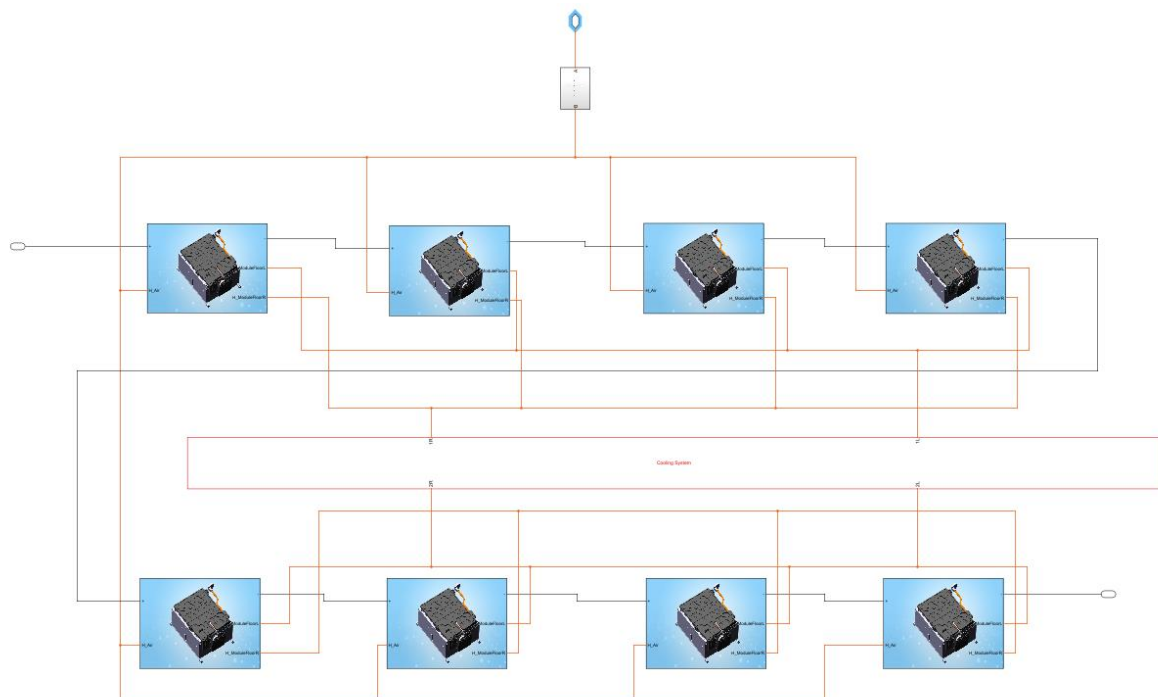


Appendix 3: Screenshots of the model in Simulink

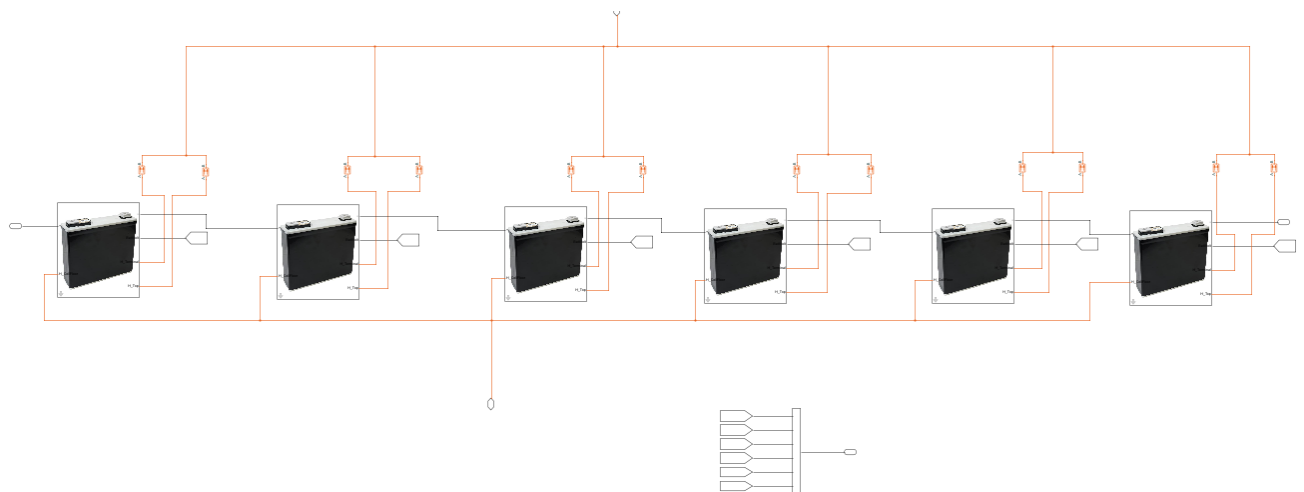
Screenshot of the pack in the model



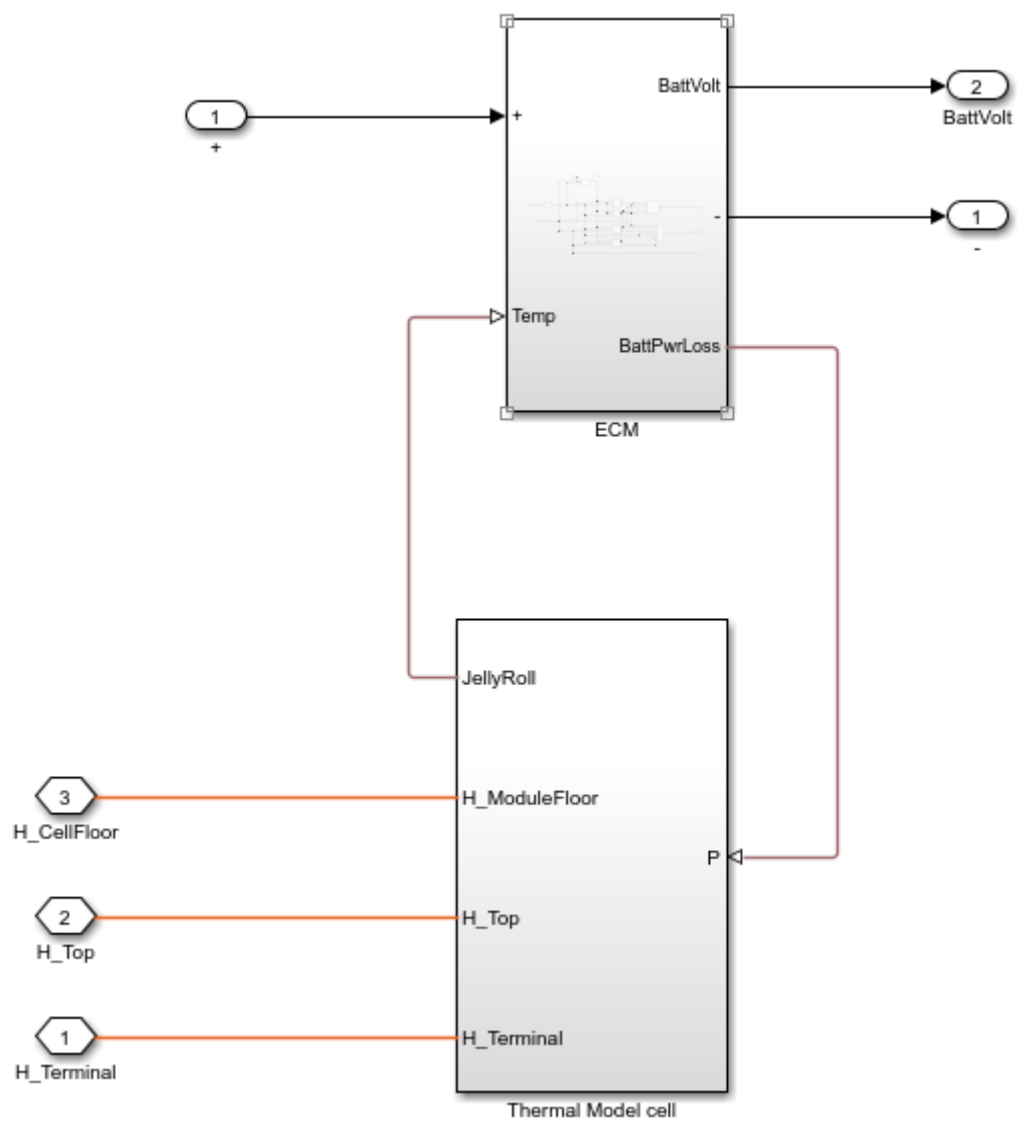
Screenshot inside the modules inside the pack



Screenshot of inside a module with only 6 cells



Screenshot of inside a cell





MÄLARDALENS HÖGSKOLA
ESKILSTUNA VÄSTERÅS

Box 883, 721 23 Västerås **Tfn:** 021-10 13 00
Box 325, 631 05 Eskilstuna **Tfn:** 016-15 36 00
E-post: info@mdh.se **Webb:** www.mdh.se